POLITECNICO DI TORINO
Repository ISTITUZIONALE

Current and emerging trends in polymeric 3D printed microfluidic devices

Original
Current and emerging trends in polymeric 3D printed microfluidic devices / Gonzalez, G.; Roppolo, I.; Pirri, C. F.; Chiappone, A.. - In: ADDITIVE MANUFACTURING. - ISSN 2214-8604. - ELETTRONICO. - 55:(2022), p. 102867. [10.1016/j.addma.2022.102867]

Availability:
This version is available at: 11583/2968086 since: 2022-06-16T15:49:20Z

Publisher:
Elsevier B.V.

Published
DOI:10.1016/j.addma.2022.102867

Terms of use:

This article is made available under terms and conditions as specified in the corresponding bibliographic description in the repository

Publisher copyright
Elsevier postprint/Author's Accepted Manuscript

© 2022. This manuscript version is made available under the CC-BY-NC-ND 4.0 license http://creativecommons.org/licenses/by-nc-nd/4.0/.The final authenticated version is available online at: http://dx.doi.org/10.1016/j.addma.2022.102867

(Article begins on next page)

12 October 2024

Current and emerging trends in polymeric 3D printed microfluidic devices

Gustavo Gonzalez [a], Ignazio Roppolo [a,b,c *], Candido Fabrizio Pirri [a,b,c], Annalisa Chiappone [d]

[a] *Department of Applied Science and Technology, Politecnico di Torino, C.so Duca Degli Abruzzi 24, 10129, Turin, Italy*
[b] *Center for Sustainable Future Technology @Polito, Italian Institute of Technology, Via Livorno 60, 10144, Turin, Italy*
[c] *PolitoBIOMed Lab, Politecnico di Torino, C.so Castelfidardo 30/A, 10129, Turin, Italy*
[d] *Dipartimento di Scienze Chimiche e Geologiche, Università di Cagliari, Complesso Universitario di Monserrato, S.S. 554 bivio Sestu, 09042 Monserrato, Italy*

** email: ignazio.roppolo@polito.it*

Abstract

During the last two decades, 3D printing technology has emerged as a valid alternative for producing microfluidic devices. 3D printing introduces new strategies to obtain high precision microfluidic parts without complex tooling and equipment, making the production of microfluidic devices cheaper, faster, and easier than conventional fabrication methods such as soft lithography. Among the main 3D techniques used for this purpose, fused filament manufacturing (FFF), inkjet 3D printing (i3Dp) and vat polymerization (VP) are of the greatest interest since they are well-established techniques in the field and are cost-affordable both in equipment and material. However, there are still some barriers in terms of technology and materials to overtake for definitively establishing 3D printing as a truly microfluidic production method. For example, the level of resolution and precision of 3D printed microfluidic parts still does not reach the level of conventional fabrication techniques, and, from a materialistic point of view, few materials present the desired characteristics (e.g., biocompatibility, optical transparency, and mechanical properties) for target areas such as medicine, analytical chemistry, and pharmaceuticals. This review intends to evaluate and analyze the current state of polymeric 3D printing techniques and materials to manufacture microfluidic chips. The article will show and discuss the latest innovations, materials, and applications of such 3D printed microstructures. The focus of this review is to provide an overview of recent and future developments in 3D printing and materials in the branch of microfluidics fabrications, showing that the selection of the right materials together with the design freedom afforded by 3D printing will be the cornerstone for microfluidic development.

Keywords: 3D printing; polymer; microfluidic; additive manufacturing; lab on a chip

1. Introduction

Over the last decades, microfluidic devices have been used for different applications, especially in chemistry and biology, introducing new analytical and laboratory procedures [1–3]. For instance, these microdevices have been applied to study cancer cells' growth and metastasis, for analyzing the interaction of such carcinogenic entities with other cells, or test and screen new types of drugs [4–7]. The interest in microfluidics lies mainly in the possibility of performing laboratory analyses on a micrometer scale, allowing savings in sample consumption, and reducing the overall costs compared to conventional laboratory procedures [8–10]. The application of these devices owed a series of benefits: high spatial resolution and sensitivity, low volume consumption, fast processing, and easiness of integration with electronic elements. Microfluidic chips are assembled with a series of sub-millimeter channels, specifically designed to achieve the desired features, e.g., mixing, pumping, or sorting the liquid passing through them [3,11–13]. By connecting such microfluidics with a few electronic elements, the devices (known as lab-on-a-chip) might be used in different biochemical applications for controlling/monitoring the behavior of specific analytical solutions, useful for rapid DNA sequencing, electrophoretic separation, wearable sensors, organ-on-chip development and disease diagnosis in point-of-care settings with a high level of precision [14–17]. The rapid deployment of microfluidic devices in laboratories and industries was marked by the introduction of polymeric materials, such as poly(methyl methacrylate) (PMMA), polycarbonate, polystyrene, polyethylene terephthalate (PET), and especially polydimethylsiloxane (PDMS). Today, PDMS elastomer is frequently used for fabricating microfluidic chips since it is an inexpensive, biocompatible, transparent, and deformable material, very suitable for molding production. For these reasons PDMS can be considered the standard material to produce microfluidic chips [18–21]. Nevertheless, PDMS presents some drawbacks, such as the non-specific adsorption of biological and chemical analytes as well as high hydrophobicity, which can be addressed with specific surface modification methods, e.g., plasma treatment, physical or chemical deposition or microwave radiation [22–30]. PDMS-based microfluidic chips are often fabricated through Soft Lithography and mold replica, a fabrication technique that involves multiple, manual, and labor-intensive steps for fabricating microfluidic devices. [31]. Other methods are micromachining, (hot)-embossing, injection molding, and laser ablation, among the principals [32–34]. Most of these methods to work properly require controlled environments or cleanroom facilities, which might not be compatible with mass production. Hence, microfluidic devices' potential growth is somehow limited to research laboratories due to the tedious and expensive fabrications methods, limiting their diffusion [35]. Therefore, more and more efforts are currently devoted to produce microfluidic devices with the right materials properties and features, by employing easier and cheaper fabrication methods, with the final goal of establishing and expanding their use and applications.

3D printing (3DP) technologies emerged as valid methods to produce fluidic devices with satisfactory results, supported by recent technological advancements in the field. 3D printing can overcome microfluidics limitations associated with mass production by enabling lower-cost and simplest fabrication of such devices in fewer steps [36–43]. 3DP, in fact, enables the on-demand production of parts from different materials that can be used in numerous industrial and research applications [44–47]. The principle behind this technology is the fabrication of three-dimensional objects from a digital model design through a single machine. The digital model (commonly in Computer-Aided Design or CAD format) is cross-sectioned by dedicated computer software. The objects are then fabricated by the selective and successive addition of material until the part is

completed. With 3DP, complex-shaped structures can be easily obtained, requiring minutes (or a few hours) without using tools, molds or complicated equipment, leading to savings in materials utilization and consumption, overall production costs, and energy, among others benefits [48–50]. Today, many different 3D printing technologies have been developed. They can be classified based on the type of material used, how materials are joined, and the working principle; each brings unique characteristics [51]. The different 3DP techniques have been extensively evaluated in multiple literature reviews, based on the type of printable material used, application areas, benefits, and drawbacks [44,51–57].

Among the different materials employed, polymeric 3DP offers multiple advantages for the medical and biomedical fields, e.g., automation, personalization, keeping relatively fast printing times, cost-affordable materials and equipment, accessibility, and high printing resolutions [58–65]. These features make polymeric 3DP a promising method for numerous biomedical applications, e.g., prototyping organ models, producing *in-vitro* platforms for cell culturing, scaffold structures for tissue engineering, on-demand fabrication of medical implants and prostheses, and multiple medical situations where it is required a fast production of customized parts [58,60,65–71]. Indeed, during the recent pandemic crisis, polymeric 3D printing demonstrated that it could be used in hospitals for the fast production of plastic valves and connectors for addressing the shortage of respiratory tools during the coronavirus disease (COVID-19) caused by the novel coronavirus (Sars-CoV-2) [72–75]. For microfluidic fabrications, not all 3D printing techniques are appropriate. Microfluidic devices should gather some essential criteria for their correct operation, such as flexibility, biocompatibility, precise design and geometry, and optical transparency, which only a few polymeric 3D printing techniques can meet. Different studies have reported the 3D printing of polymeric microfluidic devices for various *in-vitro* studies, such as bioreactors for real-time biological analysis or analytical systems [39–43]. Most of these studies are mainly focused on using methods such as (see Fig. 1) fused filament fabrication (FFF), inkjet-based 3DP, e.g., PolyJet and MultiJet, and vat polymerization methods, e.g., stereolithography (SL) and digital light processing (DLP). Several review papers have been published in the last years describing the advancements done in the development of polymeric 3D printed microfluidic chips: most of these papers analyse the literature referred to the advancements in the healthcare/biomedical field [76–78], but also different applications were reviewed[79–82]. The approach used in the most of the this literature show a technological or application-driven point of view, focusing on the different 3D printing technologies [77,83–85]. Differently, this review intends to present the updated state-of-the-art, focusing particularly on the material development, 3D printed part features such as optical transparency, printing resolution and biocompatibility, and the technological 3D printing trends considering the afore-mentioned methods. This work aims to give tools for researchers involved in microfluidic to approach more consciously to 3DP and, at the same time, for the operators of 3DP to understand the requirements of microfluidic. The most relevant applications of 3D-printed microfluidic devices are examined, highlighting the main barriers to adopt this technology in microfluidics scenarios, such as personalized medicine systems and point-of-care devices.

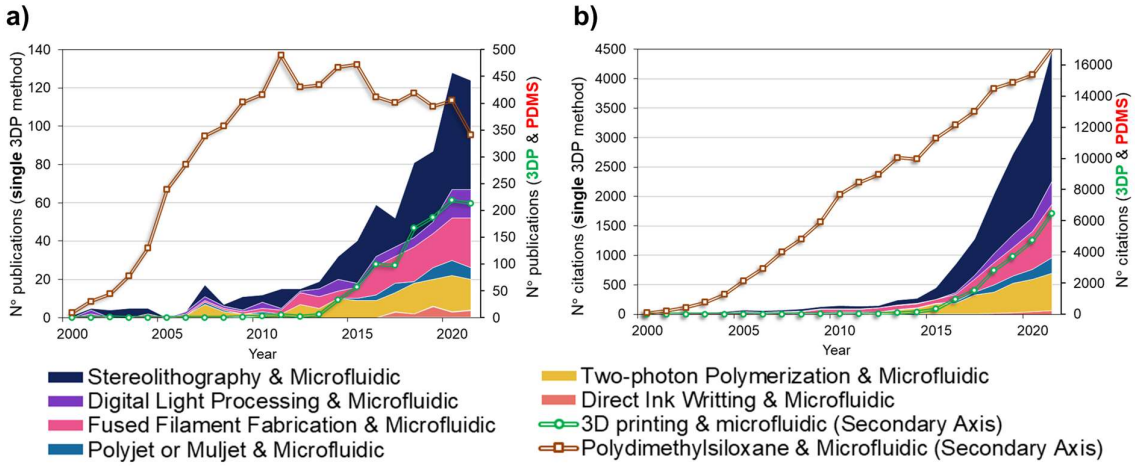

Fig. 1. Statistics data of the (a) Publications and (b) citations per year (from 2001 to 2021) searching by the keywords: "Stereolithography," "Digital Light Processing," "Fused Filament Fabrication," "PolyJet" or "MultiJet," and "two-photon polymerization" together with "microfluidic." The terms "3D printing" & "microfluidic" and "Polydimethylsiloxane" & "Microfluidic were also considered as a point of comparison. Data obtained from the Scopus database, accessed January 12th, 2022.

2. 3D printing of polymeric microfluidic devices

Numerous studies have reported the use of polymeric 3DP for microfluidic devices fabrication (see Fig. 1), showing the vast number of publications and citations per year over the last two decades using the keywords "microfluidic" and the name of a single 3D printing method [39–43,86–88]. Fig. 1.b also considers the term 3D printing to include other not well-known terms in the area of microfluidic fabrication. The acceptance of polymeric 3DP for microfluidic fabrication is evident. The number of publications in 2021 has increased more than ten times compared to 2010 and nearly four times compared to 2015. Such observation is also witnessed by the number of citations per year, which increased with *x20* and *x6* in 2020 compared to 2010 and 2015, respectively.

Interestingly, while the diagram of 3D printing and Microfluidic (both N° publications and citations per year) increases, the graph of Polydimethylsiloxane (PDMS), one of the most used materials for microfluidic fabrication start to decrease from 2010 forward. This trend is probably not only due to the appearance of 3D printing for microfluidic chip fabrication, as other microfabrication technologies and materials have appeared in recent years; however, such a trend shows that the scientific community has been searching for alternatives to conventional microfabrication methods. Most of these published works about 3D printing and microfluidic are focused on using mainly fused filament fabrication (FFF), Polyjet/MultiJet, and vat polymerization techniques, i.e., stereolithography and digital light processing, since they are well-established techniques that present a good compromise between printing resolution/accuracy, printing speed and material availability [59,89–91]. Each of the 3D printing methods offers different characteristics that can be beneficial according to the microfluidic system and its application, as summarized in Table 1. The most requested characteristics of 3D printed polymeric microfluidics are biocompatibility, optical transparency, and microchannels' reliability. The following section will present an overview of current trends and strategies to fabricate microfluidic chips by polymeric 3D printing.

2.1. Fused Filament Fabrication methods for microfluidic devices fabrication

Fused deposition modelling (FDM), also known as fused filament fabrication (FFF), is probably the most recognized 3D printing method [59,92,93]. As schematized in Fig. 2.a, in these 3D printing techniques, the material (filament) is extruded through a nozzle by thermal effect. Other extrusion-based 3D printing techniques (known as Direct Ink Writing –DIW) follow a similar extrusion-processing principle, although they use a screw, piston, or pneumatic force (pressurized air or gas) to deposit the material [52]. In general, extrusion-based 3D printing consists of a motorized system with a three-axis motion that allows material deposition selectively. The material is first deposited at the preferred position in the *XY* plane to achieve the first layer. Then a second layer is deposited onto the prior one by either the building platform moving down or the extrusion nozzle moving up; the process is repeated until the final part is obtained [94]. The fused deposition modeling (FDM) technique was invented by Scott Crump in 1989 [54,95], and after the patent expired in 2009, people started to fabricate FDM printers independently without compensating *Stratasys* (the company that branded the FDM technique), decreasing equipment and materials costs. However, *Stratasys* is still proprietary to the FDM acronym, so these methods are generally recognized as Fused Filament Fabrication (FFF) [96]. The success of FFF methods lies in their larger palette of available printable materials (see Table 1), their relatively lower cost and their more user-friendly systems and software. FFF works by heating thermoplastic filaments (linear macromolecules) through a heated nozzle above their softening point (glass transition/melting point according to the material). The softened material is deposited onto the build platform, following the computer specifications, and then cooled down [97].

Table 1. Comparison of the Fused Filament Fabrication (FFF), Polyjet/Multijet and Vat-Polymerization (VP) 3D printing in terms of microfluidic chips fabrication. The table compares the different methods of energy required to join materials (energy source), materials used, minimal printing features, smallest channel achieved, building speed, multi-material ability and pros/cons [52,69,98].

3D printing technique	**General characteristics**					**For microfluidic manufacturing**		
	Printing principle	Material	Finest machine resolution	Advantages	Disadvantages	Smallest channel achieved	Benefits	Drawbacks
Fused Filament Fabrication (FFF)	A nozzle gun builds objects by layering softened/melted wires; the objects are then hardened by cooling down	Polylactic acid (PLA), Acrylonitrile-butadiene-styrene (ABS), Polycaprolactone (PCL), Polymethylmethacrylate (PMMA), Polyurethane (PU), Polystyrene (PS), Polycarbonate (PC), Polyether ether ketone (PEEK), cyclic olefin copolymer (COC), polypropylene (PP), polyglycolic acid (PGA), polyethylene terephthalate (PET), Polyamide, polyurethane (TPU)	10-20 µm [99,100]	Low cost; A vast range of processable thermoplastics; simplicity; open-source machines; inexpensive materials; functional objects from common plastics; high printing speed	Low level of precision; Nozzle clogging; anisotropy of the printed parts; only thermoplastics materials; weak mechanical properties; rough finish; weak interlayer bonding	40 µm [101]	Cost-affordable material per printed chip. Some materials present good biocompatibility	Limited printing precision; resolution limited by nozzle diameter; Limited optical transparency; surface roughness might alter fluid flow
Polyjet/MultiJet	Jetting of photopolymerizable inks and subsequent curing of the material	Photocurable resins/photopolymers. (meth)acrylate-based; liquid suspensions; elastomers and ceramic-based inks	25 µm [102]	High accuracy, precision, and surface finishing Multi-material/color objects can be obtained	Materials are not so durable in time Sacrificial materials are difficult to recycle Post-processing might damage small features Low mechanical strength	54 µm [103]	Fast printing times, multi-material objects.	Laborious material remotion from the microchannels; No transparency parts; rough surface
Vat polymerization (VP)	Selective curing of liquid resins contained in a vat.	Photocurable resins/photopolymer. (meth)acrylate-based; epoxy; pristine acrylic resins; elastomers and ceramic-based formulations; composites and hybrid photopolymers	0.6-2 µm [104,105]	High accuracy and resolution; using flexible resins; smooth surface finish; versatility on raw material preparation; processing complex nanocomposites	High costs; low printing times; Require support; post-processing to remove support; require post-curing; limited choice of materials; difficult to produce multi-material parts	18 µm [43]	High printing resolution, fast printing chip times, good surface finishing; direct printing of fluidic channels	Post-treatment to remove unreacted material from channels and supports Cytotoxicity Limited materials

The resolution and performance of FFF methods depend on various parameters, such as temperature, the viscosity of the extruded filament, layer height, layer density, shear force, nozzle diameter printing velocity and type of material. Hence, it is essential to balance these printing parameters to reach reliable printing resolutions and accuracy and avoid defects during the 3D printing step. Today, FFF-based 3D printers can be found with a printing resolution of 10 μm, a building size as large as 200 x 200 x 400 mm^3, and a building speed as high as 500 mm/s [99,106]. The most common issue between FFF users is the inadequate adhesion between layers, leading to objects with poor mechanical properties. Such phenomenon occurs when some printing variables, such as the temperature of the processing, the temperature of the build platform (creating thermal shrinkage), and physicochemical properties of the material (e.g., heat transfer), are not well balanced [94]. Another common shortcoming of FFF methods is the lack of mechanical strength of the molten thermoplastic (it might not support itself during slow cooling) [52]. Indeed, some FFF machines use a secondary filament to support the object temporarily. This support material can be later removed by immersion in water or other types of solvents. Other drawbacks of FFF-based 3D printing are the vertical anisotropy, step structured surface (meaning low superficial resolution), layer adhesion between layers, porosities or air trapped between layers and nozzle clogging [97].

In FFF-3D printing methods, more than one nozzle can be used in the same printing process. Each nozzle can be loaded with different materials, enabling the manufacture of multi-material structures that display different properties and features in a single 3D printed object [107]. The printable filaments can also be loaded with fillers, fibers, dyes, and other additives (e.g., carbon black, glass fiber, carbon fiber and metallic powders), looking to impart specific characteristics. Various thermoplastic polymers with different features can be used in FFF-based 3D printing. The most common thermoplastics materials are polystyrene (PS), polycarbonate (PC), acrylonitrile-butadiene-styrene copolymers (ABS), polymethylmethacrylate (PMMA), polylactic acid (PLA), polyetheretherketone (PEEK), poly-ε-caprolactone (PCL), and Polyamide or Nylon; few of them with biocompatible properties [94,96,108–111]. Fig. 3 shows the chemical structure of commonly used thermoplastics for FFF-3D printing. An alternative method to FFF printing is Direct Ink Writing or DIW, in which a paste is printed (Fig. 2.b-d) [112,113]. This technique can use air pressure, a piston, or a screw to extrude the material onto the build platform. In this case, the solidification of the material can be achieved by thermal effect, photopolymerization, chemical crosslinking, rapid phase transition, and fast solvent evaporation rate, and instead of printable filaments, the DIW technique uses viscoelastic materials (or inks) with suitable rheological properties. The rheological properties of the printable ink should guarantee continuity of extrusion and be self-consistent to ensure the correct piece formation during the layer-by-layer step [114]. Typical DIW inks are made of polymers mixed with suitable organic solvents or water to adjust the viscosity of the printable material. Besides, inks of high-molecular-weight oligomers or pastes with high inorganic material content can be used [115]. DIW can process various materials since many available polymers exhibit good rheological properties. In addition, DIW can be set with multiple dispensers and composite inks, allowing multi-material and functional structures fabrication. The most used materials for DIW are silicone elastomers, polyurethane, fluorinated polymers, cellulose and gelatin-based (see Fig. 3), hydrogels polymer-based colloids, nanocomposite (e.g., graphene oxide, carbon nanotubes, silver nanowires or MXenes) and even biological material (in this case, the printing techniques are better referred to as bioprinting) [116–122].

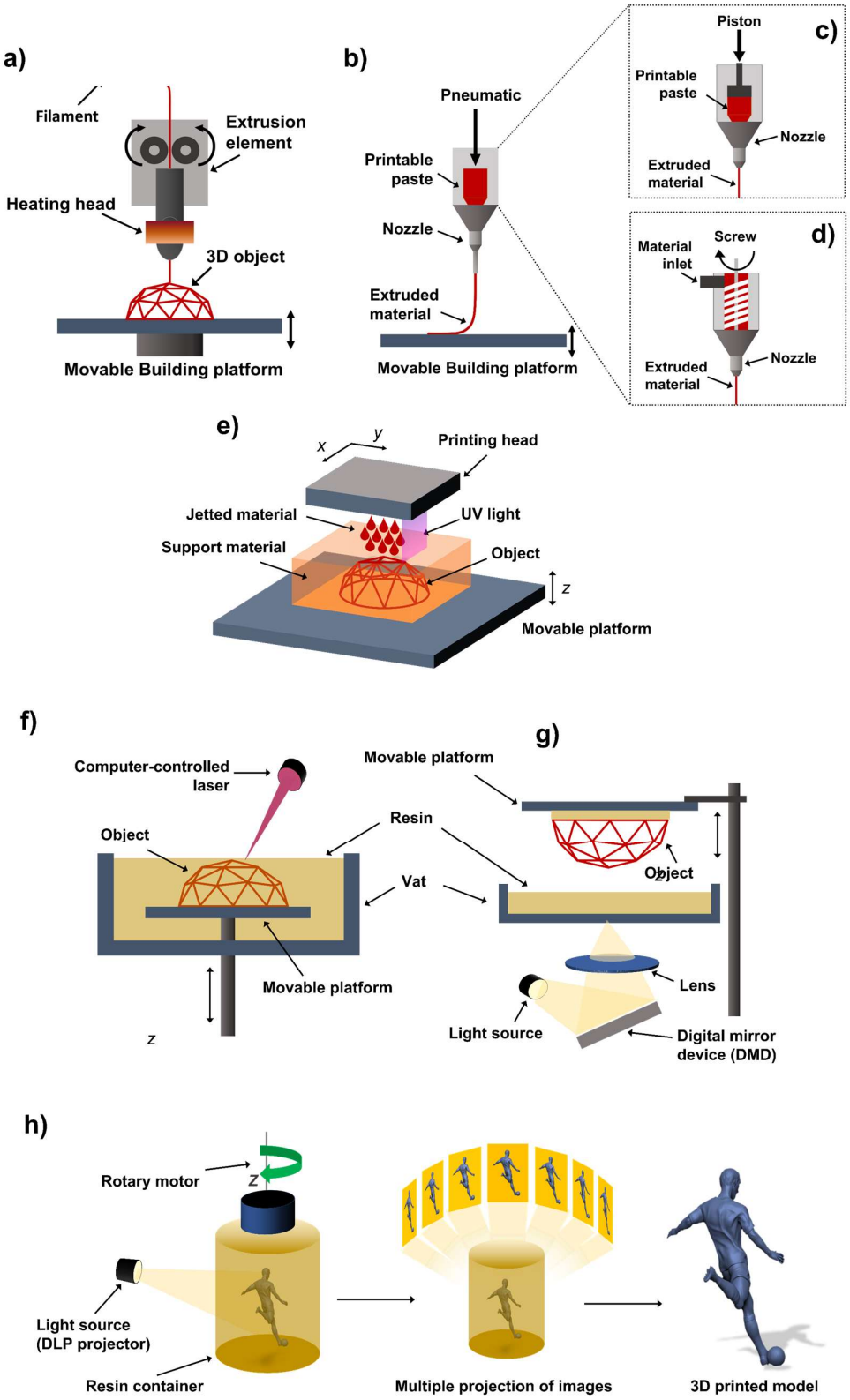

Fig. 2. Representation of (a) Fused filament fabrication (FFF), Direct ink writing based on (b) pneumatic force, (c) a piston and (d) a screw to extrude the material, (e) Photopolymerization-based inkjet 3D printing, (f) Stereolithography (SL), (g) Digital light processing (DLP) and (h) Computed axial lithography (CAL) methods.

One of the main disadvantages of DIW is the low printing velocity and resolution. In optimized conditions, the DIW can reach a printing resolution in the order of micrometers, but on the other hand, the printing time increases [118]. The highest DIW printing speed reported to date is 100 mm/s, far below the speed of other printing techniques for polymers [54]. FFF methods offer microfluidic chip fabrication benefits, such as cost-affordable materials and equipment, high printing speed, and standardized and user-friendly apparatus. Moreover, many commercially available and biocompatible filaments can be processed for microfluidic chip fabrications. The first approach involves the use of 3D printing of filaments to build the negative molds to fabricate microfluidics by casting of PDMS. In this context, it is worthy to mention the pioneering work of Saggiomo and Velders [123]. Although this method was widely explored by researchers, this is out of the scope of this review, which aims at reporting direct 3D printing of microfluidics. Through FFF methods, interesting fluidic devices have been created with satisfactory results in transparency, resolution, and biocompatibility. For example, Bressan et al. developed 3D-printed microfluidic chips based on polylactic acid (PLA) to synthesize silver and gold nanoparticles [124,125]. By optimizing the printing parameter, the chips were fabricated with channels as small as 260 μm x 260 μm employed to well-control the fluid flow behavior for obtaining particles with the desired features. These particles were then used for biological applications such as crystal violet (CV) through SERS analysis or to improve the electrocatalytic capability of carbon paste electrode (CPE) for the electrochemical determination of gallic acid (GA) and thiocyanate ions. During FFF printing processes, the wall surfaces of the printed parts can be rough due to the deposition of melted filaments. Therefore, channels with a well-established sidewall dimension are quite challenging to produce with such a 3D printing technique.

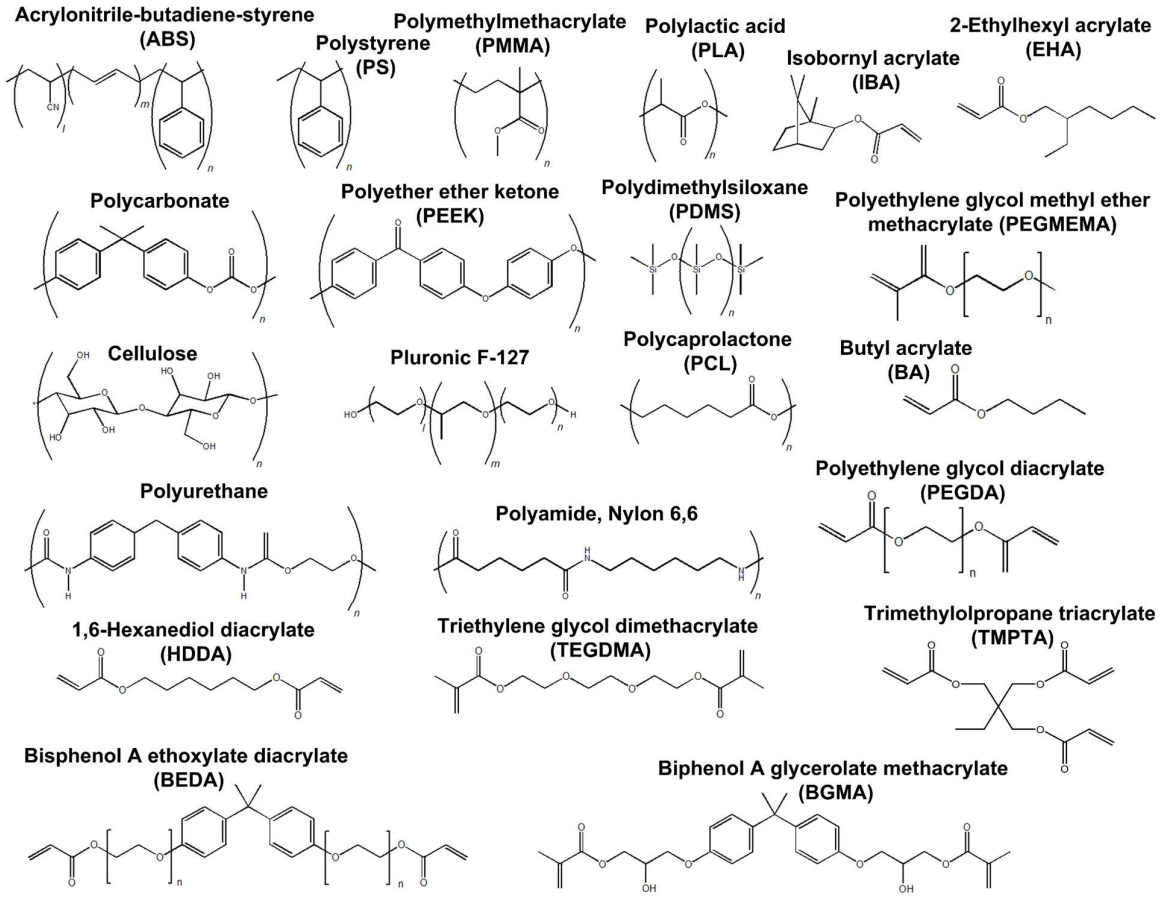

Fig. 3. Chemical structure of some commercially available polymers (thermoplastics and thermosets) used for polymeric 3D printing.

During FFF printing processes, the filament deposition can influence the walls' features, producing uneven surfaces. Therefore, channels with a well-established sidewall dimension are quite challenging to produce with FFF printing technique. Though, such surface characteristics might be used as an advantage for fluid mixing, since the surface roughness can alter the fluid behavior during the flow [126]. For example, Li et al. demonstrated how the extruded filament orientation could enhance fluidic behavior control [127]. They developed various microfluidic chips (channels of 500 μm x 500 μm) with different printing orientations of the filament (0°, 30°, 60°, and 90°) respecting the fluid flow direction to examine the fluid mixing performance (Fig. 4.a). These chips were produced with good optical transparency using a commercial filament, Crystal Clear acrylonitrile-butadiene-styrene (ABS) from *3D Systems*. Li and coworkers showed that in microfluidic chips, where the extruded filament was oriented at 60° to the flow direction, the mixing of fluids in laminar flow was achieved without any complex channel geometry or other passive mixers. Moreover, the authors demonstrated that chips' mixing performance could be adjusted by changing the filament orientation at 0° and 90°. The researchers performed simple colorimetric assays to measure the content of iron in environmental water samples, where is desired a mixing property.

The fabrication of truly microfluidic devices (<100 μm) is still challenging using FFF-3D printing. The typically requested microchannel dimensions are much smaller than most extruded filaments

and nozzles available today. Moreover, another shortcoming of FFF-3D printing is that only a few thermoplastic filaments might be used to produce optically transparent structures, which is one of the most requested characteristics of microfluidic devices for allowing the correct real-time visualization of the fluids. Some interesting strategies have been followed in this sense. For example, Kotz and coworkers produced transparent chips using commercially available polymethylmethacrylate (PMMA) filament, one of the most used materials for microfluidic chip fabrication [128]. With PMMA filaments (from *Material4print*), the authors created chips with a minimum channel width of about 300 μm x 300 μm. The chips' bottom transparency (the region of interest for proteins patterning) was significantly improved by directly printing onto PMMA sheets (not created by FFF 3d printing). These chips were used for mixing dyed water. The chip's surface was then selectively photopatterned with fluorescently labeled biotin (F5B), showing the easy biofunctionalization of 3D printed closed PMMA chips (Fig. 4.b). Similar work was presented by Bressan et al. by directly printing PLA filaments onto PMMA sheets, obtaining 3D printed microdevices with transparent bottoms [129]. The authors produced complex-shaped microfluidic devices with microchannels dimensions as narrow as 200 μm x 200 μm and with an optically transparent window in a single printing step that can be applied to perform a series of chemical measurements and visualize Saccharomyces cerevisiae microorganisms. Transparent microfluidic chips were also obtained from Nelson et al. using a commercial thermoplastic polyurethane filament (SainSmart Clear flexible TPU) [101]. They developed microfluidic chips with optical transparency (up to 85 % of transmission), chemical solvent stability, high-pressure resistance, and flexibility (see Fig. 4.c). The printed chips' biocompatibility was demonstrated by culturing mouse inner medullary collecting duct cells (mIMCD3). The researchers produced microfluidic chips with channel features as small as 50 μm x 50 μm (the smallest one by FFF to date) in less than 25 minutes. Other researchers developed transparent and sealed microfluidic chips with PLA as an alternative to conventional polydimethylsiloxane material (PDMS), acting as an electronic tongue (e-tongue). These flexible and interdigitated microfluidic chips could distinguish tastes below the human threshold. The chips were built within less than one hour, using a homemade 3D printer [130]. In addition to PLA, other types of cost-affordable materials can also be used. As reported in 2018 by Romanov and coworkers, 3D printed microfluidic chips with a channel dimension of about 400 μm were produced with either polylactic acid (PLA) or polyethylene terephthalate glycol (PETg) through two different types of commercially available low-cost FDM-3D printers: Prusa i3 ($ 600) and LulzBot ($ 2500) [131]. Such devices presented high-pressure, heat resistance, and glass-like layer characteristics, features that were useful for DNA melting analysis and facilitated the optical visualization of fluids in droplet generation and tracking and identifying DNA. Direct ink writing (DIW) methods have also been used for fabrication microstructures or microfluidic devices.

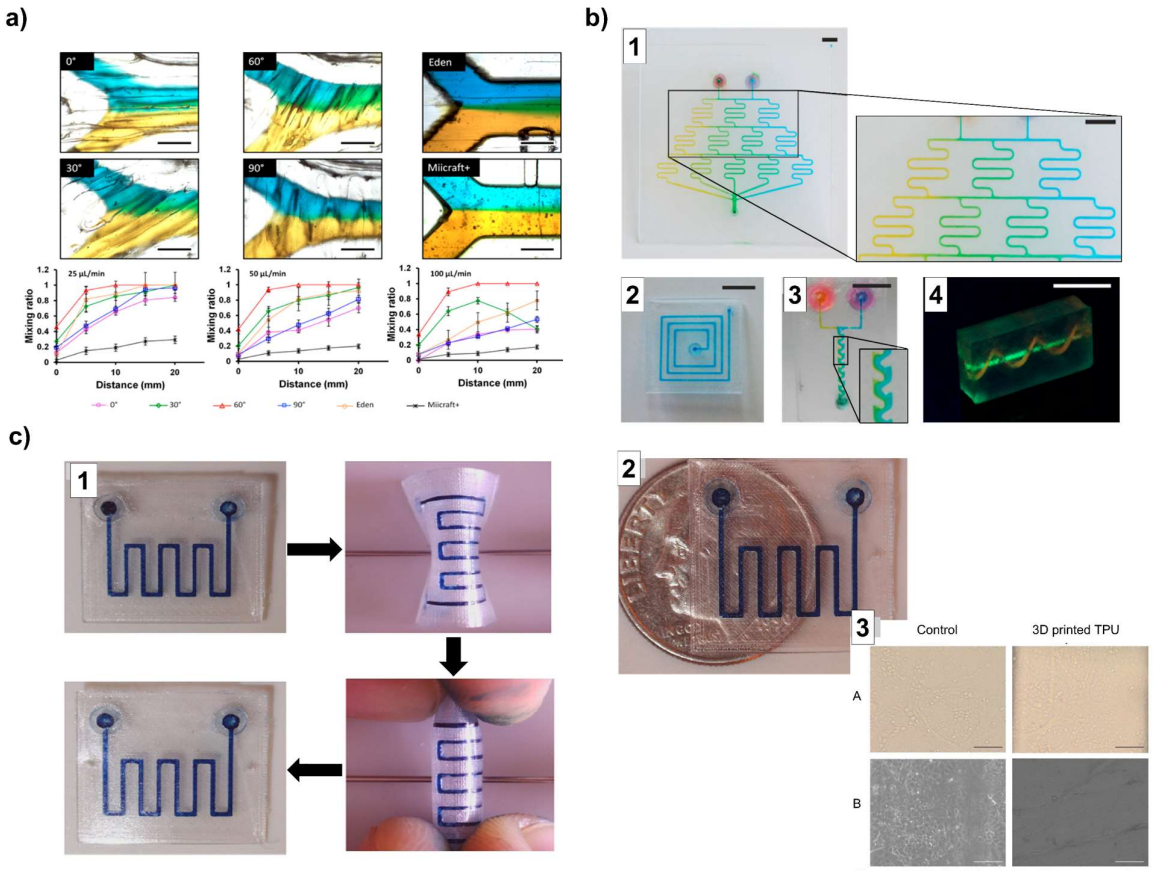

Fig. 4. 3D printed microfluidic chips fabricated by Fused Filament Fabrication (FFF)-3D printing. (a) Microscopic photographs of the laminar fluid flow inside 500µmx500µm channel toward a 750µmx500µm channel, where yellow/blue dyed water is passed through microfluidic channels fabricated by FFF methods at 0°,30°,60°, and 90° of filament orientation. The results were compared with chips produced using Eden (Polyjet) and Miicraft+ (DLP-SL) printers. Plots of distance vs. mixing ratio demonstrated the diffusion through the laminar flow channel at 25, 50, and 100 µL/min. Reprinted with permission from Ref. [127] (b) 3D printed chips in PMMA: 1) Microchip cascade for mixing yellow/blue-dyed water, 2) chip with a square channel of 600 µm x 600 µm, 3) improved mixer structure of 600 µm x 600 µm channel, and 4) 3D printed serpentine-liked channel produced around a straight channel, containing an aqueous fluorescent dye. Images with a scale bar of 10 mm. Ref. [128]. (c) Transparent 3D printed microfluidic chips made of polyurethane (TPU) images showing 1) the flexibility, 2) the chip transparency, and 3) mIMCD3 cells behavior where a characteristic cobblestone appearance was observed in both, control wells, and 3D printed TPU (scale bars = 100 µm). Reprinted with permission from Ref. [101].

Ching et al. introduced a method for fabricating microfluidic devices by directly depositing the extruded filament material onto a flat substrate using a commercial desktop DIW-3D printer [132]. The material used was a commercial silicone elastomer (Silicone sealant, Wet Area Speedseal®) patterned onto a sheet of polymethylmethacrylate (PMMA). Once the machine sketched the microchannel features, a second PMMA was used to close the device; then, a laser created the inlets and outlets elements. By intercalating multiple PMMA sheets between each printed silicone microstructure, the authors produced 3D networks of microchannels. Through such DIW method, the researchers could select the substrate (i.e., PMMA) with the required characteristics such as optical transparency and biocompatibility. Additionally, Ching and coworkers were able to willfully deform the microchannel to control the channel dimension (owing the elastomeric characteristics

of the material), reaching features as small as near 32 μm (in width) and 20 μm (in height). Through this approach, the authors pointed out three key beneficial points for the manufacturing of microfluidic chips: (1) the possibility of tuning channel dimensions, (2) the possibility of incorporating diverse types of substrates, according to the looked-for characteristic, and (3) the possibility of integrating fluid-handling and functional components such as valve and pumps in the same 3D printing process. However, the method proposed by Ching et al. requires certain manual labor to thread the PMMA sheets during 3D printing. On the other side, this method does not require removing supporting material from the microchannels, which could be a great advantage when handling fragile or delicate microfluidic systems. Athanasiadis et al. developed a DIW-based strategy to produce filaments with an internal microfluidic channel [133]. They used the 3D printer (3D discovery bioprinter, Regen HU) to first deposit a filament made of silicone elastomer (polydimethylsiloxane, SE1700 from Dow Corning) and then modify the just deposited filament with the same printing nozzle, used as a "pencil," to remove part of the material. The authors set the correct printing parameters (i.e., pneumatic pressure, nozzle diameter, nozzle heigh, and extrusion speed) to perform the post-extrusion modification and create groove-shaped filaments. Programming the stylus nozzle position above the substrate, the groove depth increase making collapse the groove walls, closing it and producing the channel. The width of the groove depends on the external diameter of the printing nozzle, which in the case of the authors was 430 μm. Even though such a strategy allowed the creation of fibers with microfluid channels), the channel dimension depended on the external diameter of the nozzle. Hu et al. described an easy way to produce PDMS-based microfluidic chips using a 3D printed sacrificial microstructure [134]. The researchers used a 3D-plotter (EnvisionTEC) to pattern the material on a PDMS substrate in a petri dish, creating fugitive or sacrificial microstructures for PDMS casting. The material was the water-soluble Pluronic F-127 ink that, once is plotted on the substrate surface, the microstructure was encapsulated with PDMS by casting. By this strategy, microdevices with channel widths varying from 300 to 570 μm were obtained by setting the right printing parameters. The Pluronic F-127 material contained inside the channels was removed, after the PDMS curing, by constantly flushing cold water and ethanol. Such a hybrid manufacturing approach allowed the authors to produce flexible, transparent, and low-cost microfluidic devices used to acetylate various amines through microwave irradiation, obtaining acetamides in shorter reaction times and good yields than conventional chemical methods. Looking for an easier integration of microfluidic devices in laboratory analysis and applications, some researchers have focused their work on creating polymeric micropumps through 3D printing [135]. Alvarez-Braña et al. created a set of polymeric micropumps using different materials, geometry, and 3D printing fabrication techniques. The authors presented the production of different self-powered modular micropumps using FFF (and other techniques such as SLA, DLP) printing techniques, studing their performance when integrated into a portable and low-cost microfluidic cartridge. In the works, the authors showed the great benefits of 3D printing in developing modular micropumps (with cylindrical cavities of 800 μm in diameter and 4 mm in depth), especially when these microparts are designed with a geometry that cannot be produced by conventional techniques. The micropumps were designed and fabricated to create autonomous flow microsystems when these are assembled with common microfluidic devices. The researchers also demonstrated that the 3D printed micropumps were responsible for the movement of the liquid through the microchannels by generating a negative pressure in the channel. Such pressure from the micropumps can be tuned according to suction properties and air absorption surfaces of the microfluidic material. The authors demonstrated the potentiality of their 3D printed micropumps by assembling them into a polymeric microfluidic cartridge to carry out a self-powered microfluidic device for colorimetric starch detection,

introducing innovative elements for the development of integrated microsystems for applications such as rapid analysis at the point-of-care.

2.2. Inkjet-based 3D printing method (i3Dp)

Inkjet-based 3D printing, i.e., Polyjet and MultiJet, is a method that employs photocurable resins deposited selectively on a platform drop-by-drop, as schematized in Fig. 2.e [136]. After the deposition of the first layer, a UV lamp, located inside the machine chamber, rapidly cures it. The platform stage is lowered, and the next film is built, repeating the process until obtaining the final structure. During the i3Dp, a blade can be used to smooth the surface of the just printed layer to guarantee a clean and uniform layer before the light-curing phase.

Polyjet 3D printing technique was invented in the latest '90s by Object Ltd (now Stratasys), being nowadays one the most commercially available 3DP methods. While in 1996, 3D Systems presented their material jetting method commercialized as MultiJet printing [137,138]. A common configuration of these printing techniques consists of various jetting heads, a three-axis motion platform, and the UV-curing device. In most of the Inkjet-based 3D printing methods, the jetting of material can be achieved by two modalities: continuous inkjet (CIJ) and drop-on-demand (DOD) [139,140]. In the CIJ-based methods, the photopolymer is continuously jetted through the nozzle by pressure action, generating a stream of droplets according to the Rayleigh-Plateau instability phenomenon of the liquid column, as described by others works [141,142]. In the DOD-based methods, the pressures pulse generates the droplets, and when this pulse exceeds the threshold at the nozzle, the droplets are ejected. Commonly, the velocity of droplets generation with CIJ-based 3D printing methods is higher than DOD-based ones with >10 m/s and 5–8 m/s, respectively [141]. The printing resolution of the inkjet-based technique is limited to hundreds of micrometers, depending on factors such as droplet diameter, the impact of the droplets onto the platform, the contact angle between the droplet and the substrate [137,141]. During a typical i3D printing condition, the printer heads spray two different materials: the building and support/sacrificial materials (used to maintain the just deposited and still liquid building material) [139,143]. In Polyjet, this sacrificial material combines acrylate monomers and other elements such as polyethylene and propylene that can be removed after the printing step by high-pressure waterjet or solvent dissolution. In MultiJet, the sacrificial material is a wax composition that is melted in a dedicated post-printing process. Both building and sacrificial material should present two crucial requirements for i3Dp use: (i) appropriate fluid properties to guarantee droplets' correct formation and precise deposition (low-viscosity materials are preferred) and (ii) high photopolymerization (curing) rate to polymerize the deposited material fast, avoiding losing the structure shape [54].

In general, i3Dp formulations are made of a mix of monomers and oligomers, photoinitiators, dyes and other additives. Monomers and oligomers are reactive polymers with functional groups (unsaturated functional groups or C=C) necessary to create the polymeric network. The chemical structures of the most common monomers and oligomers used are depicted in Fig. 3. The backbone of these reagents defines the polymerized part's final physical and mechanical properties (together with the appropriate adhesion between cured layers). Photoinitiators are compounds that absorb part of the incident light, generating reactive species or radicals through chemical transformations. These species interact with monomers and oligomers, enabling the photopolymerization mechanism [144,145]. Table 2 shows the most typical photoinitiators used for 3D printable photopolymers preparation. Dyes or pigments are organic or organometallic molecules used to

control the light's penetration during 3D printing (*Z-axis*) to enhance the printing resolution (*X-Y plane*) [146]. Other additives can be combined with printable ink, such as reactive diluents used to adjust the material's viscosity or enhance the solubility of other components such as photoinitiators or dyes [147,148]. Nano-fillers such as silica or clay fillers can also be combined with the printable ink (according to the nozzle diameter and final viscosity of the ink) to enhance the specific characteristic of the final parts, such as the mechanical properties [149].

For microfluidic chips fabrication, photopolymer-based i3Dp is preferred over other material jetting techniques such as thermal-curing-based since they combine the benefits of lithographic methods (e.g., high spatial resolution, high feature definition and good surface quality) and high build speed, material versatilities and large build volume from material jetting techniques [102]. Using Polyjet or Multijet-based printing methods, the printed microchips' surface features could be significantly enhanced compared to FFF-3D printing (although the prices are typically higher than FFF methods). Moreover, with these i3Dp methods, the printing speed and the microfluidic chips' accuracy can be higher in all axes to the extrusion-based techniques [150]. Lee et al. reported microfluidic chips by Polyjet with a nominal *X-Y* plane and *z* dimensions of 500 μm and 100 μm, respectively, with an average deviation (between the printed part and the CAD design) of 25.2 μm and with smoother features (surface roughness of 0.47 μm) compared to 67.8 μm of average deviation and 42.97 μm of surface roughness of FFF-3D printed parts (Fig. 5.a) [151]. These microfluidic chips, made from commercial material (FullCure, *Stratasys*), presented high cell viability toward C2C12 cells as a function of an appropriate post-printing sterilization step.

Table 2. Most common type I and II free radical photoinitiators for photopolymerization-based 3D printing.

Compound name	Type [a)]	Structure	Range of absorption (nm)
2-hydroxy-2-methyl propiophenone (HMMP)	I	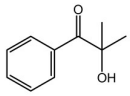	(320-360) [152]
2,2-dimethoxy-2-phenylacetophenone (DMPA)	I	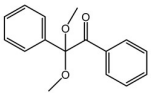	(310-370) [153]
Diphenyl(2,4,6-trimethylbenzoyl)-phosphine oxide (TPO)	I	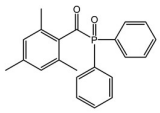	(350-410) [154,155]
phenyl bis (2,4,6-trimethylbenzoyl)-phosphine oxide (BAPO)	I	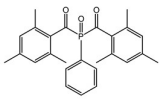	(360-440) [154]
lithium phenyl-2 4 6-trimethylbenzoyl phosphinate (LAP)	I	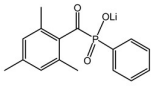	(340-400) [156]
Benzophenone	II	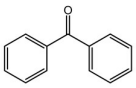	(230-280) [157]

2-Isopropylthioxanthone (ITX)	II	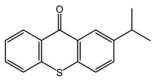	(320-400) [158]
Camphorquinone (CQ)	II	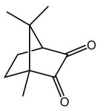	(420-490) [159]

[a)] Type I photoinitiators are compounds that undergo homolytic bond cleavage when absorbing photons, generating two free radicals from Norrish type I reactions and inducing the polymerization process. Type II photoinitiators are uncleavable organic molecules that have a more complex initiating mechanism. These bimolecular photoinitiators, upon light irradiation, can abstract hydrogen atoms from a hydrogen donor to produce excited complexes for initiating the polymerization.

Sochol et al. developed advanced components used as fluidic capacitors, diodes, and transistors to construct integrated fluidic circuits (IFC) [160]. The components were fabricated using a commercial material, Visijet M3 Crystal from 3D Systems (see Fig. 5.b), presenting limited biocompatibility. Indeed, the investigators evidenced that further works are required using more biocompatible material for Multijet printing, such as MED610, or performing the appropriate post-processing steps to provide higher biocompatibility to the chips. The authors produced reliable and sophisticated chips in which the functionalities could be customized by modifying the geometric parameters. Sweet and coworkers' work produced a series of finger-powered actuator (FPA) prototypes using Visijet material through Polyjet 3D printing [161]. The pulsatile fluid motion capability of the fabricated devices was used as modular models for microfluidic actuation and mixing purposes in an integrated fluidic platform; see Fig. 5.c. A further advantage of inkjet-based 3D printing is that it allows the fabrication of multiple microfluidic chips contemporaneously with high precision and accuracy. Walczak et al. presented the manufacturing of a series of microfluidic chips (up to 170 chips) during a single 3D printing process. The chips with diameter dimensions of 400 μm and semi-transparent features were used for capillarity gel electrophoresis. After optimizing the printing parameters in terms of printing orientation, fluorescence detection of DNA was possible [162].

In terms of optical transparency, highly transparent chips with intricate microchannels can also be produced using Polyjet for fluid mixing and optical analysis. The fluid profile of microfluidic systems is in a laminar flow; therefore, mixing different fluids efficiently and rapidly in this regime is a fundamental aspect of microfluidic chips for biological and chemical applications [163–165]. Enders et al. produced different micro-passive mixers through Polyjet methods with great optical features and sophisticated channel paths to study and compare the mixing performances between each configuration (Fig. 5.d) [166]. The designs of the most diffused mixer types, e.g., Caterpillar, enhanced Caterpillar, Tesla-like, and HC mixers, were produced using an acrylate-based material (VisiJet M2R-CL, 3D System). After a series of experimental and simulation comparison tests, they observed that Tesla-like and especially HC chips were the most suitable for the rapid and efficient mixing of fluids such as CHO-K1 (Chinese hamster ovary) cells.

The resolution of the i3Dp is generally higher than extrusion-based methods; however, it is still challenging to obtain sub-100 μm channels since this technique requires using a support material to avoid filling the built microchannel during printing. The removal of the support material after printing implies complex post-printing treatments [43,63,167]. This setback could become even trickier when the microfluidic channel configuration increases the complexity and geometry. In this context, Castiaux and collaborators proposed an interesting strategy: instead of using conventional

support material, the researchers stopped the printing process at a certain point to incorporate either a thin polycarbonate membrane or a liquid (composed of glycerol/isopropanol 65:35 v:v) as a physical barrier that can support the additional printed layers [103]. Both techniques demonstrated to be useful for creating complex-shaped microfluidic chips with channels dimensions as small as 15x250 µm, dimensions difficult to achieve by using conventional support material. However, the results obtained appear difficult to reproduce since the 250 µm x 15 µm channel was initially intended to be 125 µm x 54 µm according to their CAD design. Besides, it must be considered that stopping the printing procedure for placing extra material manually inevitably introduces additional labor in the process. One advantage of the i3Dp is its multi-material versatility by spraying various materials with different characteristics, e.g., mechanical or optical properties, during the same printing process [52,168]. Taking advantage of this characteristic, S. Keating et al. reported the 3D printing of multi-material valves using both rigid (VeroWhitePlus, RGD835, Stratasys) and flexible (TangoPlus, FLX930, Stratasys) materials. They compared the multi-material valves with single material valves observing that the former presents a more robust capability to deformation, enabling better and precise control of fluids, leading to automated production of microfluidic devices (Fig. 5.e) [169]. Keating and coworkers reported that such multipurpose fluidic chips with channels 800 µm x 800 µm and programmable valves might be used for various advanced biological applications such as DNA assembly and analysis, continuous sampling sensing, and soft robotics.

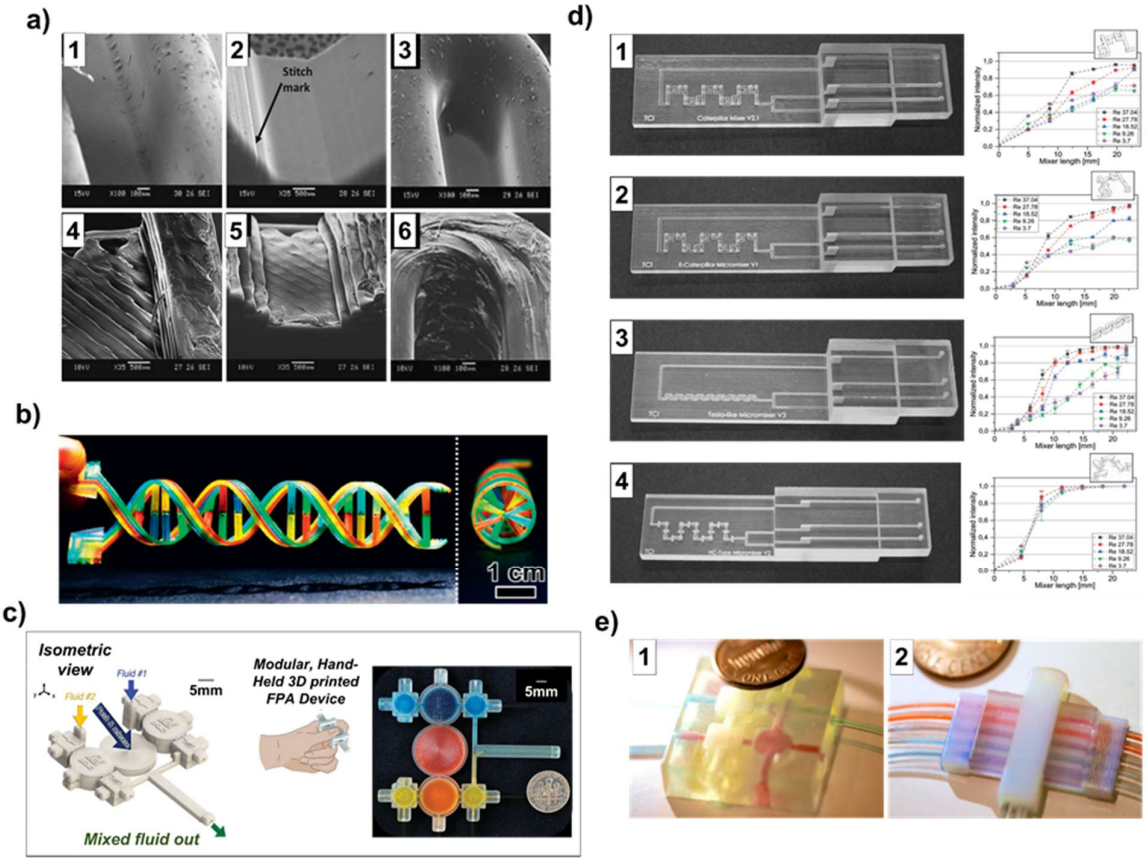

Fig. 5. 3D printed milli- and microfluidic chips fabricated by photopolymer-based inkjet 3D printing methods. (a) Scanning electron microscope (SEM) images of microchannels obtained by i3Dp (1-3) compared to microchannels obtained by FFF (4-6), showing the surface roughness between both techniques. Reprinted with permission from Ref. [151]. (b) 3D printed DNA-inspired fluidic devices are

composed of eight fluidic channels (750 μm in diameter) filled with different dye-colored solutions. Adapted with permission from Ref. [160]. (c) Working principle representation of a finger-powered two-fluid FPA prototype for fluid mixing of two distinct dyed-colored solutions. Adapted with permission from Ref. [161]. (d) Photographs of the 3D printed microfluidic mixers: 1) Caterpillar mixer, 2) enhanced Caterpillar mixer, 3) Tesla-like mixer, and 4) HC mixer. Next to each image is shown the calculated mixing performances (from simulation tests) as a mixer length function. Reprinted with permission from Ref. [166]. (e) 3D printed microfluidic multichannel valves made of 1) a single material and 2) a multi-material. Ref. [169].

Hence, the i3Dp techniques can be used for microfluidic chip fabrication with remarkable results, even if this technique requires a considerable post-printing process to clean the microchannels without damaging the microdevices correctly. Other aspects to consider are that i3Dp presents a relatively high initial cost in equipment and consumables. Besides, the window of available materials for i3Dp is limited since they are restrained by the range of viscosity and high curing rate other liquid properties (e.g., ink surface tension) requirements. Moreover, the printable materials are "regulated" formulations, developed only by the owners and therefore difficult to modify or adjust. Finally, more in-depth studies about the biocompatibility of the printable inks are still missing [58,102].

2.3. Vat polymerization method

Vat polymerization (VP) 3D printing is another photopolymerization-based technique that involves using a vat containing a liquid photopolymer [170]. This technique presents valuable features for microfluidic chips fabrication, e.g., high printing resolution and accuracy, faster printing times, and more flexibility in material tailoring and development than other polymeric 3D printing techniques (see Table 1) [90,170–174]. The VP-3D printing technique was introduced in the early '80s when the stereolithography (SL) method was developed by Hideo Kodama and Charles Hull works [175,176]. In the following years, various SL-based methods were developed, e.g., Digital Light Processing (DLP) [59,177], Micro-Stereolithography 3D printing (μSL) [178], Continuous Liquid Interface Production (CLIP) [179,180], Two-Photon Polymerization(2PP) [181], and Computed Axial Lithography (CAL) [182]. The stereolithography (SL) method is based on the selective polymerization of photopolymers by using a laser beam focused on the liquid photopolymer, as represented in Fig. 2.f. The polymer is formed by moving the laser over the resin surface (usually using a galvanometric head to control the laser) to create the first layer [183]. This polymerized layer remains attached to the building platform that is lowered according to the layer slicing step. The subsequent layers are 'printed' following the same procedure until the complete fabrication of the object. The printed parts are subjected to post-curing processes to reach the highest chemical conversions possible [68]. SL machines can be configured either top-down (Fig 2.f) or bottom-up approaches [172]. In the top-down configuration, the light comes from above, and the platform is submerged in the liquid as the part is created. While in the bottom-up, the laser beam hits the resin from the bottom of the vat through a transparent window, and the object remains attached to the platform that rises according to the formation of each layer. Generally, the bottom-up approach is preferred over the top-down since it is not dependent on the vat depth, and it requires less printable material (since it is not necessary to fill the entire vat to print).

With SL-3DP, printing features below 10 μm can be achieved [184]. At the beginning of the 90s, a derived SL technology was created, the micro-stereolithography 3D printing (MSL o μSL) with a

laser spot of about 5 μm [178]. Through μSL-3D printing, structures with sub-1 μm as a minimum feature size can be achieved [185]. Another SL-based is the Digital Light Processing 3D printing (DLP™). The DLP-based 3D printers are built by deformable mirror device (DMD) chips produced by Texas Instruments (see Fig. 2.g) [186,187]. In these configurations, each micromirror on the DMD represents one pixel in the digital image, which can drive to printing resolutions of 3 -5 μm in the *X-Y* plane according to the optical setup [188]. In the DLP-3D printing configurations, the parts are produced by projecting an entire cross-section of the object (plane-by-plane approach) rather than drawing it by a laser (line-by-line) as the case for SL methods. The photopolymerization of an entire cross-section of the object can significantly reduce printing times compared to SL techniques. Currently, commercial DLP-based printers present printing resolutions as small as 40 x 40 μm [177]. A variation of DLP-3D printing is the CLIP method which stands for Continuous Liquid Interface Production. CLIP-3D printing allows the continuous fabrication of objects by creating a thin interfacial layer of oxygen through an oxygen-permeable window. This thin oxygen layer (a dead zone) inhibits the free-radical polymerization only in the interface between the polymer film and the transparent window. Therefore, the just-built film does not adhere to the vat bottom; and the printing speed increases considerably up to hundreds of millimeters per hour. With the CLIP approach, large-scale and complex-shaped structures can be produced, maintaining high resolution [179,180]. Other light-based 3D printing methods have been developed in recent years, such as two-photon polymerization (2PP) or Computed Axial Lithography (CAL). The 2PP method is also based on a laser that scans a photopolymer [188]. The main peculiarity of the 2PP is that the process is activated by almost simultaneous absorption of two photons, which starts the free-radical polymerization, allowing polymerization control in the range of nanometer. [181,189] Some of the common drawbacks of 2PP are the limited dimensions of fabrication (no more than 1 mm height) and the lower printing velocity, which is about 0.5-1 mm/s, compared to some SL techniques (200-300 mm/s) [190]. Besides, 2PP requires expensive equipment to set the optical arrangement [191]. Many researchers have been employed 2PP as a complementary tool to produce nanometric-scale structures, which can be integrated into microfluidic devices. The idea of producing a single microfluidic device that can be easily handled in laboratories using 2PP is still far from being a reality, so this technique will not be discussed in this review. Computed Axial Lithography (CAL) is a volumetric configuration developed as an alternative to the layer-by-layer 3D printing approach [182]. CAL methods are based on computed tomography (CT) scans to generate a hologram within a controlled photopolymer volume, as shown in Fig. 2.h [192]. This hologram is created by the simultaneous projection of multiple 2D images while the vat container is rotating. The 2D images propagate through the liquid resin from different angles, resulting in a three-dimensional hologram with enough energy to photocuring, at once, a volume of photopolymer [193]. A fundamental parameter of CAL techniques is the rotation velocity that might directly influence the printing features when the rotary system is not in sync with the projected images. Another parameter of CAL is finding and adjusting the resins' viscosity since it must be high enough to avoid the relative shift between the 3D printed model and the rest of the liquid resin. CAL techniques' advantages are related to great production speed and surface definition, and these techniques can polymerize high viscosity resins (up to approximately 90 000 cP) that are difficult to achieve with other techniques such as DLP or SL [194].

In all these SL-derived 3DP techniques, the printing part enters into contact with the liquid during the printing process. Hence, one crucial point is that the polymerized object is insoluble in the liquid resin, i.e., the cured structure remains dimensionally and mechanically invariable when contacting the liquid resin. Such a condition is achieved by using cross-linkable photopolymers and

supplying the system with sufficient light energy to reach the material's gel point (the point where the liquid system starts to show more solid-like mechanical features, becoming insoluble) [170]. As for inks used in i3Dp, photopolymer for VP-3D printing combines, typically, three main chemical components: monomers/oligomers, photoinitiators, and additives. These formulations are mainly based on free-radically polymerizable resins, more frequently (meth)acrylate functionalities characterized by unsaturated C=C double bonds [195]. Such reactive groups are employed since they present high reactivity upon light irradiation, well-established mechanisms of reactions, and a wide range of (meth)acrylate-based are commercially available [196]. A few examples of the most used (meth)acrylate-based monomers and oligomers are depicted in Fig. 3. Other functionalities can also be employed, such as unsaturated polyester, vinyl, vinyl ether, thiol-ene/yne, and even cationic-based systems (in combination with free-radical systems) [197–200]. In general, the selection of suitable monomers or oligomers for vat polymerization is based on the specific application and the processing technology to be used. The main criteria are the resin functionality (mono-, di- or polyfunctional-), viscosity, reaction kinetic, hydrophobicity/hydrophilicity, shrinkage, costs, shelf life, volatility, toxicity, and the final mechanical and functional characteristic of the polymerized product [201]. As photoinitiators, different chemical compounds can be used and can operate in different electromagnetic spectrum wavelengths, e.g., UV, visible, and NIR [202–207]. These compounds can be divided into Type I (which directly generate the initiating species) and Type II (which needs a co-initiator to generate the initiating species) photoinitiators (see Table 2) and have been widely explored in the literature, and most of them can be found commercially [208–218]. However, developing more efficient photoinitiators is still of great scientific interest nowadays [219–225]. Free-radical photoinitiators are the most common substances employed in light-based 3D printing. Selecting an appropriate photoinitiator is crucial for the correct production of structures by 3D printing. The absorption spectrum of the photoinitiator must match the emission light from the printer's light source [59]. Other additives can be added to the formulation, e.g., dyes, reactive diluents or fillers to improve features or functionalities of the printed parts [146,226–233]. Many researchers find VP-3D Printing a flexible technique since, being an open technique, it can be possible to modify or adjust the liquid resin willfully [59,68,234].

In the microfluidic field, VP-3DP found applications some years ago to fabricate templates for PDMS casting for photo-lithography procedures [235,236]. Although this approach led to interesting microfluidic parts, they still present a component of manual labor (not automated) that could introduce high levels of uncertainty or errors in microfluidic assays a posteriori. One of the reasons for using VP-3DP for microfluidic devices fabrication is the possibility of producing microchips in a single step of fabrication (or in the fewest possible steps) [237]. The printable materials used should satisfy some basic criteria in the microfluidic field, e.g., suitable mechanical characteristics, good optical transparency, water/gas permeability, and chemical resistance, and low cytotoxicity [201]. Fabricating polymeric 3D printed fluidic devices with all these features is a challenging task that has led to studying several types of printable photopolymers, ranging from commercially available photopolymers to custom-made formulations and performing adequate post-printing protocols on the parts [89,238]. Au et al., in 2014, presented one of the first attempts of using VP-3DP, producing single-step fluidic chips from a commercially available SL-3D printer (3D systems Viper) and the Somos® WaterShed XC 11122 resin (marketed as a suitable resin for obtaining biocompatible and transparent objects). [239]. The researchers produced microfluidic chips with channel dimensions down to 400 μm. Another early try was presented by Prof. Breadmore in 2014 using commercial DLP-based Miicraft (Hsinchu, Taiwan) and a colorless acrylate-based resin (from the printer owner) to fabricate enclosed fluidic devices [240]. The

Miicraft is a bottom-up machine that allowed researchers to produce visible transparent microchips within a few minutes, with channel dimensions small as 250 μm and averaging $1 per chip. These early works probably provided the real starting signal for the effective production of microfluidic devices through VP-3D printing, even the technological limitations faced at that time. Gong et al. developed, in 2015, a mathematical model and performed optical characterization on a customized photopolymer to reach the smallest possible channel dimension into a microfluidic configuration [241]. In this case, the researchers developed their photopolymer based on a low-molecular PEGDA (Mn 250 g/mol), the BAPO photoinitiator (see Table 2) and varying the dye concentration (the Solvent Yellow 14). By setting the appropriate experimental conditions (e.g., light dose, build layer thickness, and resin composition), channel sizes as small as 60 μm x 108 μm were successfully achieved. Later, in 2017, the same researcher group, led by Nordin G.P., continued their studies, achieving flow channels as small as 18 μm x 20 μm, the smallest channel achieved to date (see Fig. 6.a) [41]. In this case, the researchers developed a 385 nm-UV-3D printer and a customized PEGDA-based photopolymer with 2-nitrophenyl phenyl sulfide (NPS) as a dye. The results obtained allowed the production of microfluidic chips for various applications such as entrapping microparticles (25 μm) inside microchannels built with pillars and ridged of ~ 30 μm for instance, Fig. 6.b [242], or for the extraction and separation of preterm birth (PTB) biomarkers (ferritin) in a microchannel of 45 μm x 50 μm [243]. Parker et al. recently developed microfluidic devices with cross-section channel dimensions of ~ 50 μm for microchip electrophoresis (μCE) separation of various fluorescently labeled amino acids and biomarkers related to the risk of preterm birth (PTB) [244]. By optimizing the conditions of separations (e.g., devices layout, running buffer, and the voltages applied), the yield of separation of the printed devices was comparable to conventional material for microchip electrophoresis analysis with a limit of detection in the high picomolar (pM) to low nanomolar (nM) range; this was another example of how VP-3D printing could effectively be used for microfluidic chip fabrication.

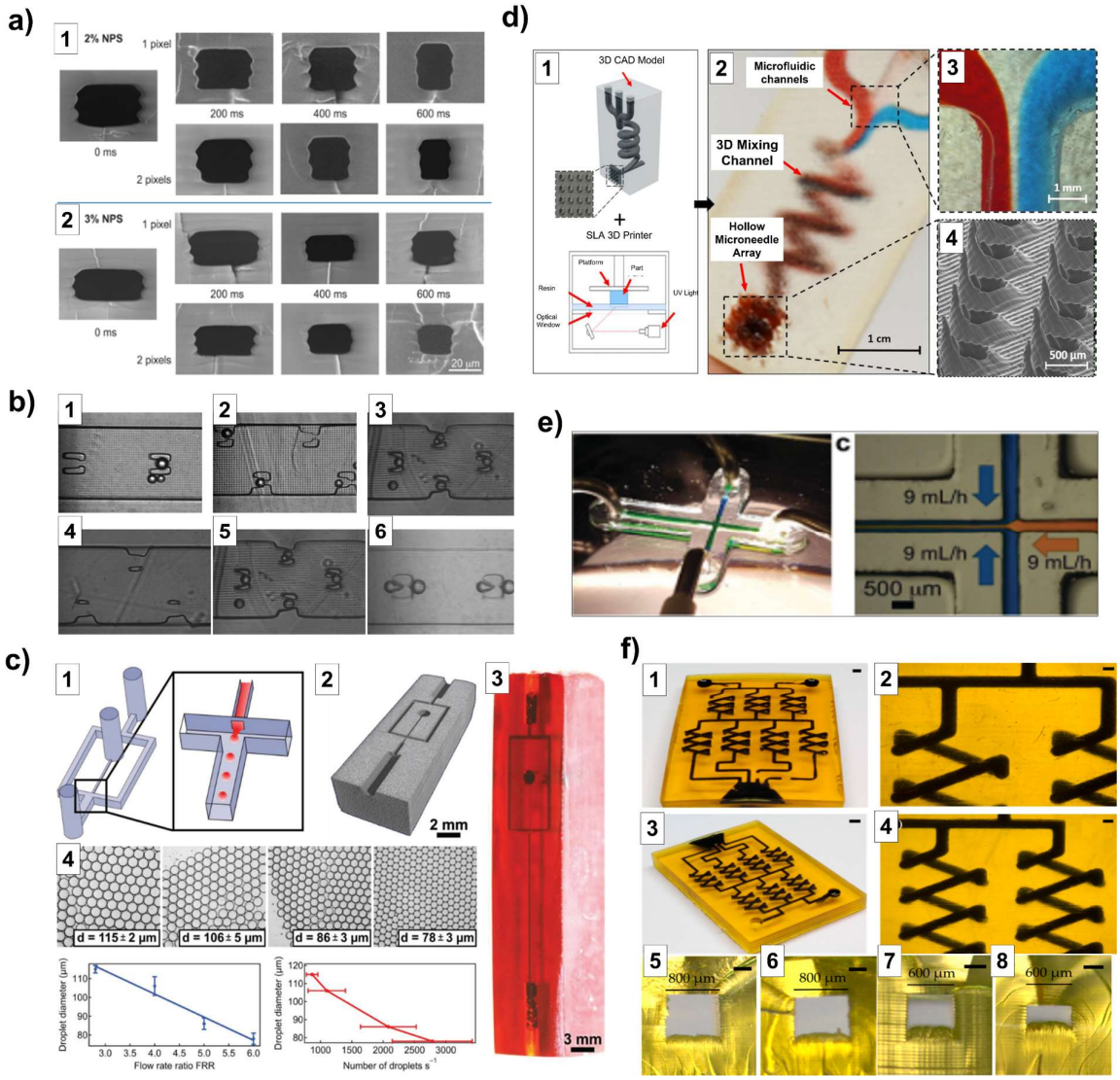

Fig. 6. 3D printed microfluidic chips fabricated by VP-3D printing. (a) 3D printed microchannels (height ~ 18 µm) using a custom-made photopolymer based on PEGDA and NPS. Reprinted with permission from Ref. [41]. (b) Photograph showing the effect of the 3D printed particles trappers positioned at different zones of a microchannel: traps positioned 1) in the center of the channels, 2) staggered along the sides of the channel, 3) staggered along the sides, and in the middle of the channel, 4) traps partially formed after 500 ms of light exposure with no bead capture, 5) particle captured in well-formed traps after 750 ms of exposure, 6) overexposed traps after 1000 ms. Ref. [242]. (c) Nonplanar 3D printed flow-focusing device: 1) representation of the microfluidic flow cell chip, 2) CAD image of the flow cell model; 3) 3D printed chip using R11 resin, and 4) diameter of the droplet generated vs. flow rate ratio (FRR) of dispersed and continuous water-oil phases. Reprinted with permission from Ref. [245]. (d) 3D printed microfluidic-enabled hollow microneedle devices: 1) CAD design and representation of the process, 2) device composed with 3) three inlets converging into a spiral mixing chamber and a 4) hollow microneedle array outlet. Reprinted with permission from Ref. [246]. (e) Microfluidic devices from a methacrylate-PDMS-based resin: 1) PDMS-based microfluidic device with 500 µm wide channels using a commercial 385 nm SL machine. 2) a central stream of yellow dye (9 mL /h) flanked by two streams of blue dye (9 mL/h each) produces a heterogeneous laminar flow (9 mL h−1) in the fluidic chip. Reprinted with permission from Ref. [247]. (f) 3D printed perfluoropolyether (PFEP) microfluidic chip: 1) front view of the gradient mixing chip (scale bar: 2 mm) with channel 2) 800 µm x 800 µm filled with black ink (scale bar: 500 µm), 3) isometric view of the gradient mixing chip (scale bar: 2 mm) with channel 4) 600 µm x 600 µm filled with black ink (scale bar: 500 µm), 5) lateral view of the 800 µm

channel width at the inlet and 6) in the middle (scale bar: 250μm), 7) lateral view of the 600 μm channel width at the inlet and 8) in the middle (scale bar: 250μm). Ref. [248].

Other important components of microfluidic chips, such as microvalves, micropumps, and other actuators, can also be produced using VP-3D printing. These components can be used to program the fluid flow and create liquid mixtures and gradients during the analysis, spearing the human labor during the tests. Gong et al. (from the G. Nordin laboratory) demonstrated reported in 2015 the production of 3D printed valves that can be driven pneumatically by willfully deflecting a thin membrane with compressed air and blocking the fluid flow [249]. These actuators were produced using a commercial 3D printer (the B9 Creator printer v1.1) and a lab-made resin based on a low-molecular PEGDA (Mn 250 g/mol), the BAPO photoinitiator and Sudan I dye. The same research group improved the stability over time of the valves and pumps, reaching performances up to 1 million of actuation [250]. Besides, the authors optimized the valve's volume (to a tenth of the original design), allowing the production of multiplexers with high-density valves integrated into microfluidic devices. The Nordin research team has been working on miniaturizing membrane-based valves and pumps with active areas as small as 15 μm × 15 μm to be integrated into 3D printed microfluidic devices [251]. Au and coworkers reported an analogous work, presenting a fully 3D printed valve that could be integrated into microfluidic systems to allow fluids' proper distribution and mixing. The model was fabricated using a commercial rewin, the WaterShed XC 11122 photopolymer (marketed as biocompatible and transparent) and the 3D systems Viper SL 3D printer machine set in high-resolution mode. The printed valve consisted of two chambers separated by a thin film or membrane: a control chamber and a fluid chamber. By flushing compressed air in the control chamber, the thin membrane deflects and remains stable, blocking the liquids off with no leaking. As a proof of concept, the research team coupled four printed valves for routing four different liquids into a 3D-printed cell culture chamber, and in this way, CHO-K1 cells were stimulated with ATP solutions, with the possibility to track their Ca2+-answer using a fluorescent dye (Fluo-4). The same group presented an article where transparent and biocompatible microfluidic chips arranged with a series of large arrays of valves were cost-affordable produced. In this case, the devices were produced using a customized photopolymer based on a low-molecular-weight (MW=258) monomer and using a commercial DLP-SL 3D printer from Asiga (Pico2-HD, 395 nm) [252].

Researchers have also been focusing more on studying the structure biocompatibility. Takenaga et al. used a commercial printer (PicoPlus 27) from Asiga and a commercial resin from the same company (PlasCLEAR) to 3D-print fluidic systems, presenting an innovative microfluidic assembly method in which the 3D printed fluidic chip is arranged on a light-addressable potentiometric sensor (LAPS) chip made from the same photopolymer. [253] The researchers used these types of assembled devices for Chinese hamster ovary (CHO)-cell growth yielding comparable results to standard cell-culture flasks and giving the possibility to monitor cells' reaction in the channels in real-time. Kuo et al. developed transparent and biocompatible microfluidic chips from a photocurable resin based on low-molecular-weight PEGDA (Mw 250), BAPO photoinitiator and the isopropyl thioxanthone (ITX) photosensitizer [254]. The ITX compound is a Type II photoinitiator that could start the polymerization process in the presence of a co-initiator. However, in Kuo et al.'s work, no co-initiators were added to the resin, and the ITX was used as a UV absorber due to the high molar absorption at 385 nm (the printer's light-emitting source). Besides, ITX neither affected the printed transparency of the microfluidic chips nor introduced unwanted coloration. The transparent chips were printed with the smallest channel width of 500 μm and having surface pillars in the order of a single-pixel (27 μm) and sub-pixel (~ 10 μm). After a post-printing process,

the printed chips' biocompatibility was tested, testing the cell viability and proliferation of the Chinese hamster ovary (CHO-K1) with promising results.

Different and interesting works were published presenting 3D printed microfluidic devices production for diversified applications. For instance, Wang et al. presented multilayered 3D microfluidic devices for flow-focusing water/oil droplet generation employing a liquid crystal display (LCD)-based SLA 3D printer [255]. However, the chips were obtained from a commercial acrylate-based resin, Spot-LV from Spot-A. The researcher opted for adding up to 2 wt.% of a green dye into the commercial photopolymer to increase the light-absorbing effect, and thus the printing resolution. They performed various tests (e.g., curing times and printing resolution in each direction) to create microfluidic chips with microchannels of 400 µm (*X-Y plane*) and 800 µm (*Z-axis*), leading to obtaining 3D printed flow-focusing droplet generators that produced droplets with sizes between 50 and 185 mm^2. Similar work was developed by Männel et al., presenting the production of nonplanar microfluidic flow cell devices for emulsion and polymeric hydrophilic/hydrophobic micro-particle formation [245]. The printed chips were produced through a commercial µSL-3DP (Perfactory P4 mini) and a commercial photopolymer (R11), both from *Envisiontec*. Printing settings such as object-resin vat separation distance, Z-axis building distance, and *X-Y* plane-light compensation at the edge's stages were adjusted to print precise microfluidic with closed channel sizes down to 75 µm in a single-fabrication step (see Fig. 6.c). The 3D printed microfluidic chips presented a similar drop-making yield to multi-step PDMS-based flow cell models fabricated by photo- and soft-lithography. Kotz et al. presented a simple method to 3D print microfluidic devices using a commercial printer (Asiga Pico 2) from a custom-made resin based on highly fluorinated (PFPE) methacrylate resin [248]. The authors selected the PFPE photocurable resin due to the high optical transparency and the polymerized parts' high chemical resistance. They opted to add into their resin two types of photoinitiator: TO and BAPO (See Table 2), and various types of light absorbers: Sudan Orange G (SOG), Tinuvin 326 (T326), and Tinuvin 384-2 (T384-2), to achieve the looked-for features. The researchers noted that the photopolymer stability was better using a SOG absorber, which also exhibits an intense absorption in the printer's light-emitting source (about 385 nm), leading to the 3D printing of embedded microfluidic chips (Fig. 6.f). As a result of the fine selection of materials, the 3D printed chips were produced with a channel width of 800 µm and a height of 600 µm as well as with high optical transparency. The printed chip presented excellent resistance toward organic solvents such as dichloromethane (DCM), N, N-dimethylformamide (DMF), tetrahydrofuran (THF) toluene, acetone, and n-heptane. In a curious work, Yeung et al. produced microfluidic chips made of an array of hollow microneedles positioned at the devices' outlet end (Fig. 6.d) [246]. The researchers employed a commercial SL-3D printer (Form2) and biocompatible material (Dental LT clear), both from FormLab. The devices were designed and printed with three separate inlet microfluidic channels that converge in one 3D spiral chamber. The incoming fluids are hydrodynamically mixed in this last chamber, emerging well-homogenized at the outlet where the microneedles (width between 800 µm and 600 µm, height below 1 mm.) are positioned. Through the channels (2 mm roughly), three-fluorochrome model-drug solutions were injected, and it was observed by ex-vivo confocal microscopy analysis that the developed devices were able to achieve the transdermal drug delivery to porcine skin. The authors reported that such systems might be applied in preclinical drug therapy situations, allowing the in-situ mixing, and tuning of multiple drugs. Many works have also been reported utilizing custom-made photopolymers as alternatives to commercial printable materials.

Other interesting works have been reported using lab-made resin based on polydimethylsiloxane (PDMS) reagents as an alternative to conventional PDMS (the Sylgard 184),

783 which is typically used for producing microfluidic chips by casting. Bhattacharjee and coworkers
784 created optically transparent PDMS-based microfluidic devices using a methacrylate-PDMS-based
785 resin and a commercial desktop-SL 3D printer (see Fig. 6.e) [247]. The printed PDMS-based devices
786 presented similar characteristics to the standard Sylgard 184 elastomer and produced chips with
787 channel dimensions down to 500 μm. Once the adequate post-printing washing steps were
788 performed, these devices presented a promising cytocompatibility toward mammalian cell lines.
789 More recently, Zips et al. presented silicone-hydrogel hybrid resins' preparation to produce flexible
790 microfluidic devices with integrated valves, mixers, and chambers through a commercial
791 stereolithography 3D printer [256]. The authors obtained microfluidic structures with internal
792 channels of 450 μm x 500 μm when the printed chip was bonded (top and down) to a glass slide.
793 As a proof of concept, the researchers used their 3D printed silicone-based microfluidic device to
794 cultivate cardiac cells (cardiomyocyte-like HL-1) in a specifically designed chamber inside the
795 printed chip, showing that the cardiac cells retained their electrophysiological activity inside the
796 silicone-based chamber. Our group recently reported the production of complex-shaped PDMS-
797 based fluidic devices by VP-3D printing [257]. The 3D printed chips were produced from a custom-
798 made photopolymer based on acrylate-PDMS, a silicone soluble BAPO-derivate photoinitiator and
799 DR1-MA as a dye, and a commercial DLP-3D printer emitting at 405 nm (Asiga PICO 2). The PDMS-
800 based chips were obtained with good optical features, high chemical stability, good mechanical
801 properties, and microchannels dimensions down to 400 μm x 400 μm. Besides, the microchannel's
802 surfaces were successfully modified, exploiting the required UV-post-curing step by taking
803 advantage of unreacted functional groups after the 3D printing step. In this way, the surface
804 properties of the PDMS-based microdevices were effectively and selectively modified through UV-
805 induced grafting polymerization techniques, giving an added value to the printed devices in terms
806 of surface treatment compared to other methods. Using continuous liquid interface production
807 (CLIP) methods, Berger and coworkers developed microfluidic devices for pathogen detection
808 [258]. The microdevices were produced using RPU70 material and the CLIP-printer Carbon M2.
809 Although with RPU70, one can produce only opaque materials, it is mechanically resistant,
810 chemically stable and compatible with various common solvents, it presents low water
811 absorptivity, and it is biocompatible (according to SO 10993-5/-10) [259]. The authors developed
812 microfluidic devices with open microchannels (or grooves) widths and depth small as 400 μm. The
813 3D printed devices were covered with transparent biocompatible tape, allowing better
814 visualization of the optical imaging during the filling. The printed chips were used to detect *E. Coli*
815 bacteria from whole blood through a loop-mediated isothermal amplification (LAMP) assay with a
816 50 cfu/μL limit of detection. The researchers reported a saponin-based lysing approach to process
817 whole blood samples directly in the chip for amplification, which subsequently allowed the
818 portable translation of the assay toward a point-of-a-care (POC) system using a smartphone.

819 3. 3D printing microfluidic chips: key-points for future improvements

820 Despite the inspiring and promising results obtained so far, there are still shortcomings that
821 polymeric 3D printing should overcome to compete with well-established techniques for
822 microchips fabrication, so to be considered a robust technology, and not just a promising
823 alternative. The most looked-for characteristics in 3D printed fluidic chips are printing resolution
824 and accuracy, optical transparency, and biocompatibility. Current commercial 3D printing
825 resolution is still lower (or poorer) than conventional lithography methods. Most of the published
826 works of 3D-printed microfluidics reported microchannels in the range of 0.5 - 1 mm. Researchers
827 have been looking for novel methods to manufacture truly microfluidic devices (<100 μm). Some

researchers achieved sub-millimeter dimension channels using not-so-quite handy and replicable methods. The truth is that these strategies are still highly experimental, and even more technological and material development is needed to converge 3D printing and microfluidic systems entirely.

The FFF method is a 3D printing technique with a high printing speed and low initial cost. Using FFF, sacrificial masters can be produced, that can be dissolved in a post-3D printing step to develop truly sub-millimeters microfluidic chips (the smallest features 18 μm using a nozzle of 30 μm of diameter) [123,260]. However, for direct FFF 3D printing of microfluidic the precision remains quite above the sub-millimeter features. As discussed previously, photopolymer-based 3D printing methods are considered the best alternative for microfluidic chip manufacturing. Inkjet 3D printing (i3Dp) presents a better printing resolution than extrusion-based techniques. However, the correct fabrication of sub-microfluidic devices is limited by the supporting material used in the fabrication step. The supporting material can be trapped inside the channels, and it can be quite difficult to remove from the microchannels. In this view, an innovative strategy was presented based on the pausing-and-printing approach by introducing a thin sheet or liquid substances as a physical barrier rather than the conventional supporting material, leading researchers to reach sub-millimeter channel dimensions through i3Dp [103]. However, this method is rather manual and depends on the correct alignment of the physical barrier. With vat polymerization techniques, larger-scale and precise microfluidic chips can be produced faster, though the transversal resolution is still to be improved [258]. The printing resolution of stereolithography and digital light processing 3D printing techniques can reach a few micrometers, although they typically present a lower printing speed than FFF and i3Dp [54]. The stringent request for the future on this side is the improvement of printing resolution to a range similar to soft lithography. This can be reached with 2PP; however, this equipment is not suitable for mass production. It is thus necessary for a synergistic improvement of machines technology, which hopefully can gather multiple technologies, and materials.

Beyond resolution, another crucial feature for the 3D printing of microfluidic chips is biocompatibility [261–263]. Among the 3D printed techniques discussed in this review, FFF is with the wider commercially available biocompatible materials, as shown in Table 1 [101,102], e.g., polylactic acid (PLA), polymethylmethacrylate (PMMA), polycarbonate (PC), cyclic olefin copolymer (COC), polypropylene (PP), acrylonitrile-butadiene-styrene (ABS) and polyurethane (TPU). These materials can also be found in the market at good prices compared to other materials used for different polymeric 3D printing methods. The situation is slightly different for photopolymerization-based inkjet and Vat polymerization 3D printing. Considering the nature of printable photopolymers, the printed objects frequently contain unreacted chemical products (monomers, photoinitiators, and additives) after the printing step. Such unreacted chemicals can be toxic to biological entities, hindering the full potential application in the biomedical field [264,265]. Many researchers have reported novel formulations using hydrogels [120,266–269]. Hydrogels' main characteristic is their great compatibility with biological entities since they are designed to uptake high water content (> 90 wt.%) [270]. These features make hydrogels attractive for medical, biomedical and pharmaceutics applications [271,272]. Though, their implementation for microfluidic devices' manufacturing has not been completely adopted because hydrogels could interact undesirably with the fluids flushing through the microchannels, leading to structural changes of the chips [267]. An aspect to consider is that the printed microfluidic devices need to operate with delicate aqueous-based analytes in cell culture or tissue engineering applications [273], which could be solved using hydrogels with partially hydrophobic characteristics [256]. On

the other hand, fluidic platforms made with more dimensionally stable and water-free polymers could enable better performance of microfluidic devices, even if the biocompatibility features are not so great as hydrogels. Recent studies have shown the importance of improving the biocompatibility of such water-free structures [273,274]. In this frame, diverse commercial photopolymers marketed as biocompatible have been reported [245,275]. However, as discussed in the review, only a few studies have been carried out related to the material-biological unit interactions. Most of the studies have been focused on Vat polymerization techniques; for instance, a detailed characterization of four commercial photopolymers (from Formlab) was carried out by Piironen et al., studying their compatibility toward cell lines [276]. The researchers concluded that even if a commercial resin is ISO-certified as biocompatible, it does not imply an adequate cell interaction of the produced parts. They observed that the most crucial point is performing a post-printing procedure on objects to remove the toxic component and improve biocompatibility. Other researchers reached a similar conclusion [277,278]. In all these previous works, the result was common: more attention must be paid to the post-printing procedures to reduce the leaching of toxic compounds from the printed parts.

Even following a post-printing procedure, the lack of detailed information from the supplier about the chemical composition of the resin further complicates the biological studies performance of the printed parts. Herein, the growing interest in developing custom-made photopolymers for 3D printing with biocompatibility features [187,279]. In this line, the idea is to formulate resins to obtain printed parts with adequate biocompatibility and reduced cytotoxicity, which could be foreseen as biocompatible materials for advanced applications after standard treatment validations [68,280]. The development of in-lab and more biocompatible materials, however, could be achieved mainly using vat polymerization techniques owing to their versatility in material preparation (while for i3Dp, producing and implementing in-house materials is hindered by the restriction level of the machines' owners). A work from Nordin's group demonstrated that printed parts (based on PEGDA, Mn 250) were noncytotoxic toward endothelial cells (EA. hy926) even without any post-printing treatment [274]. Männel et al. evaluated the biocompatibility of (meth)acrylate resins toward human umbilical vein endothelial cells (HUVECs) [273]. They tested resins such as PEGMEMA (Mn 500 g/mol), TPGDA (Mn 300.55 g/mol), POEA (Mw 192.21 g/mol) and PEGDA (Mn 575 g/mol). They noticed that a combination of PEGDA and PEGMEMA was the most suitable composition, observing a cell proliferation after five (5) days of culture. Different researchers have explored how the biocompatibility of the printed parts can be increased by removing or reducing the unreacted and potential cytotoxic products by following the appropriate post-printing steps [170,281,282]. Though, the printed objects' bio-functionality can also be enhanced by performing particular post-3D printing protocols not to remove the potentially cytotoxic components from their surface (or "passivation") but by coupling bio-functional groups on their surfaces (or "activation"). These functional groups might be active biological molecules such as antibodies, peptides, nucleic acids, or biocompatible compounds to promote biological interactions like carboxylic acid groups or thiols. As proposed by Männel and coworkers in their work, the bioproperties of 3D printed parts might be significantly enhanced if RGD tripeptides are incorporated in the photosensitive resin rather than performing post-printing procedures [273]. By adding Br-containing vinyl-terminated initiator into a commercial UV curable resin, 3D printed objects with modifiable surfaces can be obtained [283]. Such an approach promotes polymer brushes' growth via surface-initiated atom transfer radical polymerization (SI-ATRP) that can be potentially used in the biomedical field. This "activation" strategy could be an interesting path to

follow to introduce functional biomolecules that might enhance the biocompatibility or the bio-interaction of the photopolymerized printed parts with specific biological entities [284].

As seen in this review, interesting use of 3D printed microfluidic chips has been reported. The manufacturing of microfluidic devices by 3DP is still in a development phase, with some specific works reporting the biomedical and pharmaceutical application of 3D printed chips [285–289]. Many expectations are still put on polymer 3D printing due to the flexibility and versatility to simplify and decentralize the micro-manufacturing steps. We think that polymeric 3D printing will soon meet the technological innovations and materials research necessary to bridge current gaps, producing microfluidic devices for patient-specific treatment, more commonly known as Point-of-a-care (POC) devices, as illustrated in Fig. 7. Many researchers have demonstrated the use of polymeric 3D printing to produce microfluidic devices for the patient-specific detection of saliva, urine, and other biological entities. This opens up a myriad of medical applications by combining 3D printing with real medical situations. Low-cost 3D printed microfluidic devices may provide a new avenue for molecular detection at the point of care in resource-limited settings. Over time, it is certainly possible to envision a future where these facilities are shared regionally or nationally, supported by an on-call production team, to improve accessibility to these custom 3D printed and POC devices.

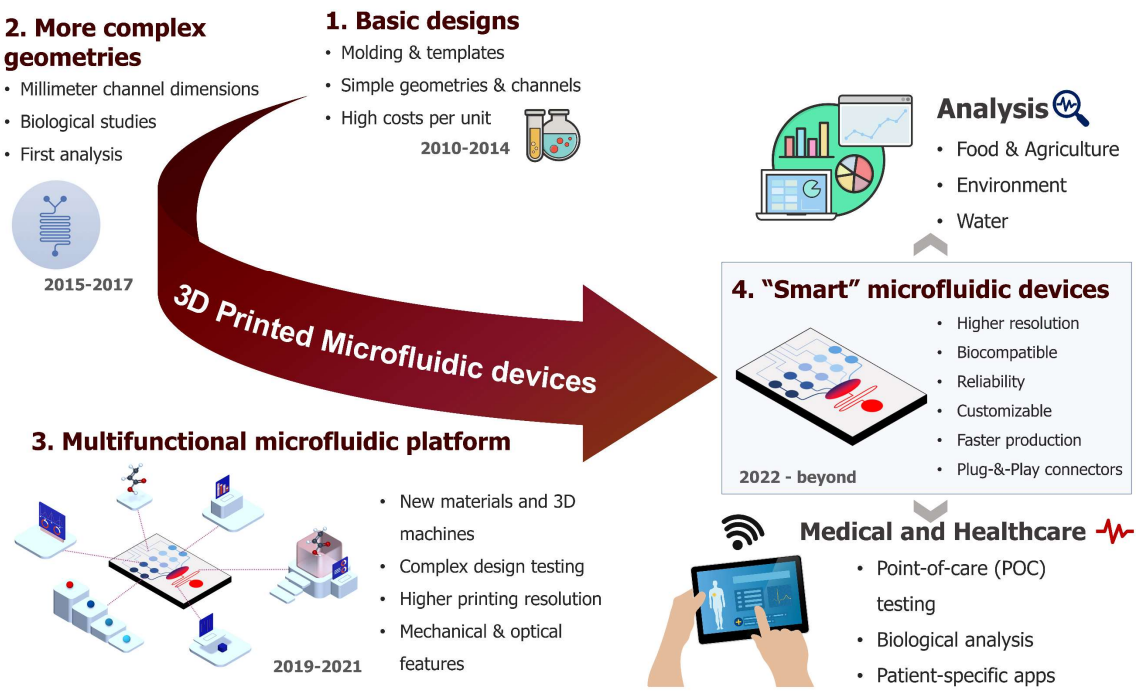

Fig. 7. Past and projection of 3D printing for microfluidic chip fabrication. 1) Basic designs: initially, 3D printing was mainly used for the production of sacrificial molds for casting fabrication techniques; 2) More complex geometries: the development of new materials and 3D printing machines and technology, more complex-shaped microfluidic chips were successfully fabricated, though most of the application were proof-of-concepts based on preliminary biochemical analysis; 3) Multifunctional microfluidic platforms: the growing interest for 3D printed microfluidic chips led researchers to develop interesting works obtaining more performance microfluidic platforms with different properties (e.g., biocompatibility and good mechanical and optical features) due to more advanced materials and 3D printing methods; 4) "Smart" microfluidic devices: the future of 3D printed microfluidic devices seems to be bright as more innovative materials and 3D printers are developed. Based on our experience, we believe that the evolution of 3D printing in the microfluidic sector might

create a future scenario where one can produce rapidly microfluidic chips for the treatment of the specific analysis and patient situations, indeed, many researchers agree in a future where 3D printing, and the microfluidic world can contribute to the developing of precise and low-cost point-of-a-care devices.

4. Conclusions

Polymeric 3D printing is a promising technology that can revolutionize the microfluidic field by introducing faster and cheaper ways to produce microdevices. These technologies, especially FFF, i3Dp and VP-3D printing, are also establishing new strategies for manufacturing such devices, new commercialization approaches, and fields of application. Although the expected potential of 3D printing, it still presents a few shortcomings that should be overcome to compete with well-established conventional techniques for microchips fabrication and thus be considered a valid technology and not just a promising alternative. In this review, an attempt was made to highlight the need to develop and improve the performance of current 3D printing materials and technologies to achieve the great potential of this technology.

In the next few years, we might expect that the progression of 3D printing will be establishing the pillars to appoint this technology as the best alternative for manufacturing microfluidic devices. To achieve such a goal, there is still so much to do in terms of materials and technology development to reach the greatest resolutions, the better precision as possible, the desired optical characteristics, and structures with higher biocompatible features. In recent years, most of the published works are more focused on presenting how polymeric 3D printing could be effectively used for microfluidic fabrication based on studying the characteristics of the machine or using or developing alternative materials. Now, it is time that the 3D printed microfluidics will be used in real microfluidic applications to start to comprehend the possible future scenarios that, in synergy with machines and software progress and material development, will lead to polymeric 3D printing the expected transformation in the field. Although the utilization of 3D printing has not yet become a central part of standard microfluidic chips today, we anticipate that given the prospects for 3D printing and continuous performance improvement, this technology will be adopted, and more opportunities will progressively emerge for companies and institutions to relevant applications in global health.

5. References

[1] P. Yager, T. Edwards, E. Fu, K. Helton, K. Nelson, M.R. Tam, B.H. Weigl, Microfluidic diagnostic technologies for global public health, Nature. 442 (2006) 412–418. https://doi.org/10.1038/nature05064.

[2] E. Verpoorte, Microfluidic chips for clinical and forensic analysis, Electrophoresis. 23 (2002) 677–712. https://doi.org/10.1002/1522-2683(200203)23:5<677::AID-ELPS677>3.0.CO;2-8.

[3] C.Y. Lee, C.L. Chang, Y.N. Wang, L.M. Fu, Microfluidic mixing: A review, International Journal of Molecular Sciences. (2011). https://doi.org/10.3390/ijms12053263.

[4] M. Zhang, C. Xu, L. Jiang, J. Qin, A 3D human lung-on-a-chip model for nanotoxicity testing, Toxicology Research. 7 (2018) 1048–1060. https://doi.org/10.1039/c8tx00156a.

[5] D. Huh, A human breathing lung-on-a-chip, Ann Am Thorac Soc. 12 (2015) S42–S44. https://doi.org/10.1513/AnnalsATS.201410-442MG.

[6] D. Huh, Reconstituting Organ-Level Lung, Science (1979). (2010) 1662–1668.

[7] Y.-H.V. Ma, K. Middleton, L. You, Y. Sun, A review of microfluidic approaches for investigating cancer extravasation during metastasis, Microsystems & Nanoengineering. 4 (2018) 1–13. https://doi.org/10.1038/micronano.2017.104.

[8] A. Bohr, S. Colombo, H. Jensen, Chapter 15 - Future of microfluidics in research and in the market, in: H.A. Santos, D. Liu, H. Zhang (Eds.), Microfluidics for Pharmaceutical Applications, William Andrew Publishing, 2019: pp. 425–465. https://doi.org/https://doi.org/10.1016/B978-0-12-812659-2.00016-8.

[9] M. Lake, C. Arciso, K. Cowdrick, T. Storey, S. Zhang, J. Zartman, D. Hoelzle, Microfluidic device design, fabrication, and testing protocols, Protocol Exchange. (2015) 1–26. https://doi.org/10.1038/protex.2015.069.

1004 [10] M. Mehling, S. Tay, Microfluidic cell culture, Current Opinion in Biotechnology.
1005 25 (2014) 95–102. https://doi.org/10.1016/j.copbio.2013.10.005.

1006 [11] C.Y. Lee, W.T. Wang, C.C. Liu, L.M. Fu, Passive mixers in microfluidic systems:
1007 A review, Chemical Engineering Journal. (2016).
1008 https://doi.org/10.1016/j.cej.2015.10.122.

1009 [12] E.A. Mansur, M. YE, Y. WANG, Y. DAI, A State-of-the-Art Review of Mixing in
1010 Microfluidic Mixers, Chinese Journal of Chemical Engineering. (2008).
1011 https://doi.org/10.1016/S1004-9541(08)60114-7.

1012 [13] D. Di Carlo, Inertial microfluidics, Lab on a Chip. 9 (2009) 3038–3046.
1013 https://doi.org/10.1039/b912547g.

1014 [14] B.M. Paegel, R.G. Blazej, R.A. Mathies, Microfluidic devices for DNA sequencing:
1015 Sample preparation and electrophoretic analysis, Current Opinion in
1016 Biotechnology. 14 (2003) 42–50. https://doi.org/10.1016/S0958-1669(02)00004-6.

1017 [15] J. Scott Mellors, K. Jorabchi, L. M. Smith, J. Michael Ramsey, Integrated
1018 Microfluidic Device for Automated Single Cell Analysis Using Electrophoretic
1019 Separation and Electrospray Ionization Mass Spectrometry, Analytical
1020 Chemistry. 82 (2010) 967–973. https://doi.org/10.1021/ac902218y.

1021 [16] S.K. Vashist, P.B. Luppa, L.Y. Yeo, A. Ozcan, J.H.T. Luong, Emerging
1022 Technologies for Next-Generation Point-of-Care Testing, Trends in
1023 Biotechnology. 33 (2015) 692–705. https://doi.org/10.1016/j.tibtech.2015.09.001.

1024 [17] G.A. Akceoglu, Y. Saylan, F. Inci, A Snapshot of Microfluidics in Point-of-Care
1025 Diagnostics: Multifaceted Integrity with Materials and Sensors, Advanced
1026 Materials Technologies. 2100049 (2021). https://doi.org/10.1002/admt.202100049.

1027 [18] S. Halldorsson, E. Lucumi, R. Gómez-Sjöberg, R.M.T. Fleming, Advantages and
1028 challenges of microfluidic cell culture in polydimethylsiloxane devices,
1029 Biosensors and Bioelectronics. 63 (2015) 218–231.
1030 https://doi.org/10.1016/j.bios.2014.07.029.

1031 [19] A. Mata, A.J. Fleischman, S. Roy, Characterization of polydimethylsiloxane
1032 (PDMS) properties for biomedical micro/nanosystems., Biomed Microdevices. 7
1033 (2005) 281–293. https://doi.org/10.1007/s10544-005-6070-2.

1034 [20] I.D. Johnston, D.K. McCluskey, C.K.L. Tan, M.C. Tracey, Mechanical
1035 characterization of bulk Sylgard 184 for microfluidics and microengineering,
1036 Journal of Micromechanics and Microengineering. 24 (2014).
1037 https://doi.org/10.1088/0960-1317/24/3/035017.

1038 [21] K. Ren, J. Zhou, H. Wu, Materials for microfluidic chip fabrication, Accounts of
1039 Chemical Research. 46 (2013) 2396–2406. https://doi.org/10.1021/ar300314s.

1040 [22] L. Yu, C.M. Li, Y. Liu, J. Gao, W. Wang, Y. Gan, Flow-through functionalized
1041 PDMS microfluidic channels with dextran derivative for ELISAs, Lab on a Chip.
1042 9 (2009) 1243–1247. https://doi.org/10.1039/b816018j.

1043 [23] Z.L. Zhang, C. Crozatier, M. Le Berre, Y. Chen, In situ bio-functionalization and
1044 cell adhesion in microfluidic devices, Microelectronic Engineering. 78–79 (2005)
1045 556–562. https://doi.org/10.1016/j.mee.2004.12.071.

1046 [24] J. Xu, K.K. Gleason, Conformal, amine-functionalized thin films by initiated
1047 chemical vapor deposition (iCVD) for hydrolytically stable microfluidic devices,
1048 Chemistry of Materials. (2010). https://doi.org/10.1021/cm903156a.

1049 [25] X. Yu, J. Xiao, F. Dang, Surface modification of poly(dimethylsiloxane) using ionic
1050 complementary peptides to minimize nonspecific protein adsorption, Langmuir.
1051 31 (2015) 5891–5898. https://doi.org/10.1021/acs.langmuir.5b01085.

1052 [26] S. Hu, X. Ren, M. Bachman, C.E. Sims, G.P. Li, N. Allbritton, Surface modification
1053 of poly(dimethylsiloxane) microfluidic devices by ultraviolet polymer grafting,
1054 Analytical Chemistry. (2002). https://doi.org/10.1021/ac025700w.

1055 [27] B.T. Ginn, O. Steinbock, Polymer surface modification using microwave-oven-
1056 generated plasma, Langmuir. (2003). https://doi.org/10.1021/la034138h.

1057 [28] A.Y.N. Hui, G. Wang, B. Lin, W.T. Chan, Microwave plasma treatment of
1058 polymer surface for irreversible sealing of microfluidic devices, Lab on a Chip.
1059 (2005). https://doi.org/10.1039/b504271b.

1060 [29] T. Goda, T. Konno, M. Takai, K. Ishihara, Synthesis and characterization on
1061 polydimethylsiloxane grafted with poly(2-methacryloyloxyethyl
1062 phosphorylcholine) by photo-induced radical polymerization, in: Polymer
1063 Preprints, Japan, 2005.

1064 [30] M.D. Kurkuri, F. Al-Ejeh, J.Y. Shi, D. Palms, C. Prestidge, H.J. Griesser, M.P.
1065 Brown, B. Thierry, Plasma functionalized PDMS microfluidic chips: Towards
1066 point-of-care capture of circulating tumor cells, Journal of Materials Chemistry.
1067 (2011). https://doi.org/10.1039/c1jm10317b.

1068 [31] J.C. McDonald, D.C. Duffy, J.R. Anderson, D.T. Chiu, H. Wu, O.J.A. Schueller,
1069 G.M. Whitesides, Fabrication of microfluidic systems in poly(dimethylsiloxane),
1070 Electrophoresis. 21 (2000) 27–40. https://doi.org/10.1002/(sici)1522-
1071 2683(20000101)21:1<27::aid-elps27>3.3.co;2-3.

1072 [32] B.K. Gale, A.R. Jafek, C.J. Lambert, B.L. Goenner, H. Moghimifam, U.C. Nze, S.K.
1073 Kamarapu, A review of current methods in microfluidic device fabrication and
1074 future commercialization prospects, Inventions. 3 (2018).
1075 https://doi.org/10.3390/inventions3030060.

1076 [33] A.G. Niculescu, C. Chircov, A.C. Bîrcă, A.M. Grumezescu, Fabrication and
1077 applications of microfluidic devices: A review, International Journal of Molecular
1078 Sciences. 22 (2021) 1–26. https://doi.org/10.3390/ijms22042011.

1079 [34] V.I. Vullev, J. Wan, V. Heinrich, P. Landsman, P.E. Bower, B. Xia, B. Millare, G.
1080 Jones, Nonlithographic fabrication of microfluidic devices, J Am Chem Soc. 128
1081 (2006) 16062–16072. https://doi.org/10.1021/ja061776o.

1082 [35] D. Mark, S. Haeberle, G. Roth, F. Von Stetten, R. Zengerle, Microfluidic Lab-on-
1083 a-Chip Platforms: Requirements, Characteristics and Applications, in: S. Kakaç,

1084 B. Kosoy, D. Li, A. Pramuanjaroenkij (Eds.), Microfluidics Based Microsystems.
1085 NATO Science for Peace and Security Series A: Chemistry and Biology, Springer,
1086 Dordrecht, 2010.

1087 [36] C. Chen, B.T. Mehl, A.S. Munshi, A.D. Townsend, D.M. Spence, R.S. Martin, 3D-
1088 printed microfluidic devices: fabrication, advantages and limitations - a mini
1089 review, Analytical Methods. (2016). https://doi.org/10.1039/c6ay01671e.

1090 [37] V. Mehta, S.N. Rath, 3D printed microfluidic devices: a review focused on four
1091 fundamental manufacturing approaches and implications on the field of
1092 healthcare, Bio-Design and Manufacturing. (2021).
1093 https://doi.org/10.1007/s42242-020-00112-5.

1094 [38] C. Su, Review of 3D-Printed functionalized devices for chemical and biochemical
1095 analysis, Analytica Chimica Acta. (2021) 338348.
1096 https://doi.org/10.1016/j.aca.2021.338348.

1097 [39] F. Zhu, A. Wigh, T. Friedrich, A. Devaux, S. Bony, D. Nugegoda, J. Kaslin, D.
1098 Wlodkowic, Automated Lab-on-a-Chip Technology for Fish Embryo Toxicity
1099 Tests Performed under Continuous Microperfusion (μFET), Environmental
1100 Science and Technology. 49 (2015) 14570–14578.
1101 https://doi.org/10.1021/acs.est.5b03838.

1102 [40] T.M. Valentin, E.M. Dubois, C.E. Machnicki, D. Bhaskar, F.R. Cui, I.Y. Wong, 3D
1103 printed self-adhesive PEGDA-PAA hydrogels as modular components for soft
1104 actuators and microfluidics, Polymer Chemistry. 10 (2019) 2015–2028.
1105 https://doi.org/10.1039/c9py00211a.

1106 [41] H. Gong, B.P. Bickham, A.T. Woolley, G.P. Nordin, Custom 3D printer and resin
1107 for 18 μm × 20 μm microfluidic flow channels, Lab on a Chip. (2017).
1108 https://doi.org/10.1039/C7LC00644F.

1109 [42] K. Alessandri, M. Feyeux, B. Gurchenkov, C. Delgado, A. Trushko, K.H. Krause,
1110 D. Vignjević, P. Nassoy, A. Roux, A 3D printed microfluidic device for production

1111 of functionalized hydrogel microcapsules for culture and differentiation of
1112 human Neuronal Stem Cells (hNSC), Lab on a Chip. 16 (2016) 1593–1604.
1113 https://doi.org/10.1039/c6lc00133e.

1114 [43] M.J. Beauchamp, G.P. Nordin, A.T. Woolley, Moving from millifluidic to truly
1115 microfluidic sub-100-μm cross-section 3D printed devices, Analytical and
1116 Bioanalytical Chemistry. 409 (2017) 4311–4319. https://doi.org/10.1007/s00216-
1117 017-0398-3.

1118 [44] T.D. Ngo, A. Kashani, G. Imbalzano, K.T.Q. Nguyen, D. Hui, Additive
1119 manufacturing (3D printing): A review of materials, methods, applications and
1120 challenges, Composites Part B: Engineering. 143 (2018).
1121 https://doi.org/10.1016/j.compositesb.2018.02.012.

1122 [45] G. Anglani, 3D printed capsules for self-healing concrete applications, (2019).
1123 https://doi.org/10.21012/fc10.235356.

1124 [46] D.S. Thomas, S.W. Gilbert, Costs and cost effectiveness of additive
1125 manufacturing: A literature review and discussion, in: Additive Manufacturing:
1126 Costs, Cost Effectiveness and Industry Economics, 2015.

1127 [47] F. Matos, R. Godina, C. Jacinto, H. Carvalho, I. Ribeiro, P. Peças, Additive
1128 manufacturing: Exploring the social changes and impacts, Sustainability
1129 (Switzerland). (2019). https://doi.org/10.3390/su11143757.

1130 [48] M. Mehrpouya, A. Dehghanghadikolaei, B. Fotovvati, A. Vosooghnia, S.S.
1131 Emamian, A. Gisario, The potential of additive manufacturing in the smart
1132 factory industrial 4.0: A review, Applied Sciences (Switzerland). 9 (2019).
1133 https://doi.org/10.3390/app9183865.

1134 [49] M. Gebler, A.J.M. Schoot Uiterkamp, C. Visser, A global sustainability
1135 perspective on 3D printing technologies, Energy Policy. (2014).
1136 https://doi.org/10.1016/j.enpol.2014.08.033.

[50] S. Ford, M. Despeisse, Additive manufacturing and sustainability: an exploratory study of the advantages and challenges, Journal of Cleaner Production. 137 (2016) 1573–1587. https://doi.org/10.1016/j.jclepro.2016.04.150.

[51] D. Chen, S. Heyer, S. Ibbotson, K. Salonitis, J.G. Steingrímsson, S. Thiede, Direct digital manufacturing: Definition, evolution, and sustainability implications, Journal of Cleaner Production. (2015). https://doi.org/10.1016/j.jclepro.2015.05.009.

[52] M. Rafiee, R.D. Farahani, D. Therriault, Multi-Material 3D and 4D Printing: A Survey, Advanced Science. 7 (2020) 1–26. https://doi.org/10.1002/advs.201902307.

[53] D.T. Pham, R.S. Gault, A comparison of rapid prototyping technologies, International Journal of Machine Tools and Manufacture. 38 (1998) 1257–1287. https://doi.org/10.1016/S0890-6955(97)00137-5.

[54] L.Y. Zhou, J. Fu, Y. He, A Review of 3D Printing Technologies for Soft Polymer Materials, Advanced Functional Materials. 2000187 (2020) 1–38. https://doi.org/10.1002/adfm.202000187.

[55] B.C. Gross, J.L. Erkal, S.Y. Lockwood, C. Chen, D.M. Spence, Evaluation of 3D Printing and Its Potential Impact on Biotechnology and the Chemical Sciences, (2014).

[56] B. Berman, 3-D printing: The new industrial revolution, Business Horizons. 55 (2012) 155–162. https://doi.org/10.1016/j.bushor.2011.11.003.

[57] J. Zhao, M. Hussain, M. Wang, Z. Li, N. He, Embedded 3D printing of multi-internal surfaces of hydrogels, Additive Manufacturing. 32 (2020) 101097. https://doi.org/10.1016/j.addma.2020.101097.

[58] N. Bhattacharjee, A. Urrios, S. Kang, A. Folch, The upcoming 3D-printing revolution in microfluidics, Lab on a Chip. 16 (2016) 1720–1742. https://doi.org/10.1039/C6LC00163G.

1163 [59] J.W. Stansbury, M.J. Idacavage, 3D printing with polymers: Challenges among
1164 expanding options and opportunities, Dental Materials. 32 (2016) 54–64.
1165 https://doi.org/10.1016/j.dental.2015.09.018.

1166 [60] M. Hofmann, 3D printing gets a boost and opportunities with polymer materials,
1167 ACS Macro Letters. (2014). https://doi.org/10.1021/mz4006556.

1168 [61] J. Ni, H. Ling, S. Zhang, Z. Wang, Z. Peng, C. Benyshek, R. Zan, A.K. Miri, Z. Li,
1169 X. Zhang, J. Lee, K.J. Lee, H.J. Kim, P. Tebon, T. Hoffman, M.R. Dokmeci, N.
1170 Ashammakhi, X. Li, A. Khademhosseini, Three-dimensional printing of metals
1171 for biomedical applications, Materials Today Bio. 3 (2019).
1172 https://doi.org/10.1016/j.mtbio.2019.100024.

1173 [62] R.D. Sochol, E. Sweet, C.C. Glick, S.Y. Wu, C. Yang, M. Restaino, L. Lin, 3D
1174 printed microfluidics and microelectronics, Microelectronic Engineering. 189
1175 (2018) 52–68. https://doi.org/10.1016/j.mee.2017.12.010.

1176 [63] S. Waheed, J.M. Cabot, N.P. Macdonald, T. Lewis, R.M. Guijt, B. Paull, M.C.
1177 Breadmore, 3D printed microfluidic devices: enablers and barriers, Lab on a Chip.
1178 16 (2016) 1993–2013. https://doi.org/10.1039/C6LC00284F.

1179 [64] R. Amin, S. Knowlton, A. Hart, B. Yenilmez, F. Ghaderinezhad, S. Katebifar, M.
1180 Messina, A. Khademhosseini, S. Tasoglu, 3D-printed microfluidic devices,
1181 Biofabrication. 8 (2016) 022001. https://doi.org/10.1088/1758-5090/8/2/022001.

1182 [65] C.M.B. Ho, S.H. Ng, K.H.H. Li, Y.-J. Yoon, 3D printed microfluidics for biological
1183 applications, Lab on a Chip. 15 (2015) 3627–3637.
1184 https://doi.org/10.1039/C5LC00685F.

1185 [66] Q. Yan, H. Dong, J. Su, J. Han, B. Song, Q. Wei, Y. Shi, A Review of 3D Printing
1186 Technology for Medical Applications, Engineering. 4 (2018) 729–742.
1187 https://doi.org/10.1016/j.eng.2018.07.021.

1188 [67] C. Lee Ventola, Medical applications for 3D printing: Current and projected uses,
1189 P and T. 39 (2014) 704–711.

1190 [68] R.J. Mondschein, A. Kanitkar, C.B. Williams, S.S. Verbridge, T.E. Long, Polymer
1191 structure-property requirements for stereolithographic 3D printing of soft tissue
1192 engineering scaffolds, Biomaterials. 140 (2017) 170–188.
1193 https://doi.org/10.1016/j.biomaterials.2017.06.005.

1194 [69] C.M. González-Henríquez, M.A. Sarabia-Vallejos, J. Rodriguez-Hernandez,
1195 Polymers for additive manufacturing and 4D-printing: Materials, methodologies,
1196 and biomedical applications, Progress in Polymer Science. 94 (2019) 57–116.
1197 https://doi.org/10.1016/j.progpolymsci.2019.03.001.

1198 [70] S. V. Murphy, A. Atala, 3D bioprinting of tissues and organs, Nature
1199 Biotechnology. 32 (2014) 773–785. https://doi.org/10.1038/nbt.2958.

1200 [71] S. Knowlton, B. Yenilmez, S. Tasoglu, Towards Single-Step Biofabrication of
1201 Organs on a Chip via 3D Printing, Trends in Biotechnology. 34 (2016) 685–688.
1202 https://doi.org/10.1016/j.tibtech.2016.06.005.

1203 [72] L. Cavallo, A. Marcianò, M. Cicciù, G. Oteri, 3D Printing beyond Dentistry during
1204 COVID 19 Epidemic: A Technical Note for Producing Connectors to Breathing
1205 Devices, Prosthesis. 2 (2020) 46–52. https://doi.org/doi:10.3390/prosthesis2020005.

1206 [73] R. Tino, R. Moore, S. Antoline, P. Ravi, N. Wake, C.N. Ionita, J.M. Morris, S.J.
1207 Decker, A. Sheikh, F.J. Rybicki, L.L. Chepelev, COVID-19 and the role of 3D
1208 printing in medicine, 3D Printing in Medicine. (2020).
1209 https://doi.org/10.1186/s41205-020-00064-7.

1210 [74] M. Salmi, J.S. Akmal, E. Pei, J. Wolff, A. Jaribion, S.H. Khajavi, 3D printing in
1211 COVID-19: Productivity estimation of the most promising open source solutions
1212 in emergency situations, Applied Sciences (Switzerland). 10 (2020).
1213 https://doi.org/10.3390/app10114004.

1214 [75] S. Ishack, S.R. Lipner, Applications of 3D Printing Technology to Address
1215 COVID-19−Related Supply Shortages, The American Journal of Medicine. 133
1216 (2020) 771–773. https://doi.org/https://doi.org/10.1016/j.amjmed.2020.04.002.

1217 [76] P. Prabhakar, R.K. Sen, N. Dwivedi, R. Khan, P.R. Solanki, A.K. Srivastava, C.
1218 Dhand, 3D-Printed Microfluidics and Potential Biomedical Applications,
1219 Frontiers in Nanotechnology. 3 (2021). https://doi.org/10.3389/fnano.2021.609355.

1220 [77] V. Mehta, S.N. Rath, 3D printed microfluidic devices: a review focused on four
1221 fundamental manufacturing approaches and implications on the field of
1222 healthcare, Bio-Design and Manufacturing. (2021).
1223 https://doi.org/10.1007/s42242-020-00112-5.

1224 [78] C.M.B. Ho, S.H. Ng, K.H.H. Li, Y.-J. Yoon, 3D printed microfluidics for biological
1225 applications, Lab on a Chip. 15 (2015) 3627–3637.
1226 https://doi.org/10.1039/C5LC00685F.

1227 [79] H. Nazari, A. Heirani-Tabasi, S. Ghorbani, H. Eyni, S. Razavi Bazaz, M. Khayati,
1228 F. Gheidari, K. Moradpour, M. Kehtari, S.M. Ahmadi Tafti, S.H. Ahmadi Tafti,
1229 M.E. Warkiani, Microfluidic-Based Droplets for Advanced Regenerative
1230 Medicine: Current Challenges and Future Trends, Biosensors (Basel). 12 (2022).
1231 https://doi.org/10.3390/bios12010020.

1232 [80] P. Prabhakar, R.K. Sen, N. Dwivedi, R. Khan, P.R. Solanki, A.K. Srivastava, C.
1233 Dhand, 3D-Printed Microfluidics and Potential Biomedical Applications,
1234 Frontiers in Nanotechnology. 3 (2021). https://doi.org/10.3389/fnano.2021.609355.

1235 [81] C. Heuer, J.A. Preuß, T. Habib, A. Enders, J. Bahnemann, 3D printing in
1236 biotechnology—An insight into miniaturized and microfluidic systems for
1237 applications from cell culture to bioanalytics, Engineering in Life Sciences. (2021).
1238 https://doi.org/10.1002/elsc.202100081.

1239 [82] L. Wang, M. Pumera, Recent advances of 3D printing in analytical chemistry:
1240 Focus on microfluidic, separation, and extraction devices, TrAC - Trends in
1241 Analytical Chemistry. 135 (2021) 116151.
1242 https://doi.org/10.1016/j.trac.2020.116151.

1243 [83] C. Chen, B.T. Mehl, A.S. Munshi, A.D. Townsend, D.M. Spence, R.S. Martin, 3D-
1244 printed microfluidic devices: fabrication, advantages and limitations - a mini
1245 review, Analytical Methods. 8 (2016) 6005–6012.
1246 https://doi.org/10.1039/c6ay01671e.

1247 [84] H. Mea, J. Wan, Microfluidics-enabled functional 3D printing., Biomicrofluidics.
1248 16 2 (2022) 021501.

1249 [85] A.K. Au, W. Huynh, L.F. Horowitz, A. Folch, 3D-Printed Microfluidics,
1250 Angewandte Chemie - International Edition. (2016) 3862–3881.
1251 https://doi.org/10.1002/anie.201504382.

1252 [86] C. Credi, G. Griffini, M. Levi, S. Turri, Biotinylated Photopolymers for 3D-Printed
1253 Unibody Lab-on-a-Chip Optical Platforms, Small. 14 (2018) 1–8.
1254 https://doi.org/10.1002/smll.201702831.

1255 [87] F. Zhu, N. Macdonald, J. Skommer, D. Wlodkowic, Biological implications of lab-
1256 on-a-chip devices fabricated using multi-jet modelling and stereolithography
1257 processes, SPIE Microtechnologies. 9518 (2015) 951808.
1258 https://doi.org/10.1117/12.2180743.

1259 [88] P. Panjan, V. Virtanen, A.M. Sesay, Towards microbioprocess control: An
1260 inexpensive 3D printed microbioreactor with integrated online real-Time glucose
1261 monitoring, Analyst. 143 (2018) 3926–3933. https://doi.org/10.1039/c8an00308d.

1262 [89] G. Weisgrab, A. Ovsianikov, P.F. Costa, Functional 3D Printing for Microfluidic
1263 Chips, Advanced Materials Technologies. 4 (2019).
1264 https://doi.org/10.1002/admt.201900275.

1265 [90] N.P. Macdonald, J.M. Cabot, P. Smejkal, R.M. Guijt, B. Paull, M.C. Breadmore,
1266 Comparing Microfluidic Performance of Three-Dimensional (3D) Printing
1267 Platforms, Analytical Chemistry. 89 (2017) 3858–3866.
1268 https://doi.org/10.1021/acs.analchem.7b00136.

[91] M. Zeraatkar, D. Filippini, G. Percoco, On the impact of the fabrication method on the performance of 3D printed mixers, Micromachines (Basel). 10 (2019). https://doi.org/10.3390/mi10050298.

[92] R. Melnikova, A. Ehrmann, K. Finsterbusch, 3D printing of textile-based structures by Fused Deposition Modelling (FDM) with different polymer materials, IOP Conference Series: Materials Science and Engineering. 62 (2014). https://doi.org/10.1088/1757-899X/62/1/012018.

[93] J. Emmermacher, D. Spura, J. Cziommer, D. Kilian, T. Wollborn, U. Fritsching, J. Steingroewer, T. Walther, M. Gelinsky, A. Lode, Engineering considerations on extrusion-based bioprinting: interactions of material behavior, mechanical forces and cells in the printing needle, Biofabrication. 12 (2020) 025022. https://doi.org/10.1088/1758-5090/ab7553.

[94] S. Vyavahare, S. Teraiya, D. Panghal, S. Kumar, Fused deposition modelling: a review, Rapid Prototyping Journal. 26 (2020) 176–201. https://doi.org/10.1108/RPJ-04-2019-0106.

[95] S. Crump, Apparatus and method for creating three-dimensional objects - Patent, 1992. https://doi.org/10.2116/bunsekikagaku.28.3_195.

[96] S. Singh, G. Singh, C. Prakash, S. Ramakrishna, Current status and future directions of fused filament fabrication, Journal of Manufacturing Processes. 55 (2020) 288–306. https://doi.org/10.1016/j.jmapro.2020.04.049.

[97] I.J. Solomon, P. Sevvel, J. Gunasekaran, A review on the various processing parameters in FDM, Materials Today: Proceedings. 37 (2020) 509–514. https://doi.org/10.1016/j.matpr.2020.05.484.

[98] X. Wang, M. Jiang, Z. Zhou, J. Gou, D. Hui, 3D printing of polymer matrix composites: A review and prospective, Composites Part B: Engineering. 110 (2017) 442–458. https://doi.org/10.1016/j.compositesb.2016.11.034.

[99] Raise3D, Pro2 Dual Extruder 3D Printer, (2021). https://www.raise3d.com/pro2/ (accessed August 12, 2021).

[100] Ultimaker, Ultimaker S3: Powerful, professional 3D printing, (n.d.). https://ultimaker.com/3d-printers/ultimaker-s3 (accessed August 16, 2021).

[101] M.D. Nelson, N. Ramkumar, B.K. Gale, Flexible, transparent, sub-100 μm microfluidic channels with fused deposition modeling 3D-printed thermoplastic polyurethane, Journal of Micromechanics and Microengineering. 29 (2019). https://doi.org/10.1088/1361-6439/ab2f26.

[102] S.C. Ligon, R. Liska, J. Stampfl, M. Gurr, R. Mülhaupt, Polymers for 3D Printing and Customized Additive Manufacturing, Chemical Reviews. 117 (2017) 10212–10290. https://doi.org/10.1021/acs.chemrev.7b00074.

[103] A.D. Castiaux, C.W. Pinger, E.A. Hayter, M.E. Bunn, R.S. Martin, D.M. Spence, PolyJet 3D-Printed Enclosed Microfluidic Channels without Photocurable Supports, Analytical Chemistry. (2019). https://doi.org/10.1021/acs.analchem.9b01302.

[104] BMF Materials Inc., Industrial Micro-Precision 3D Printers, (2020). https://bmf3d.com/.

[105] Q. Ge, Z. Li, Z. Wang, K. Kowsari, W. Zhang, X. He, J. Zhou, N.X. Fang, Projection micro stereolithography based 3D printing and its applications, International Journal of Extreme Manufacturing. 2 (2020). https://doi.org/10.1088/2631-7990/ab8d9a.

[106] WASP, Delta WASP 2040 become PRO, (n.d.). https://www.allthat3d.com/fastest-3d-printers/ (accessed August 12, 2021).

[107] D. Han, H. Lee, ScienceDirect Recent advances in multi-material additive manufacturing : methods and applications, Current Opinion in Chemical Engineering. 28 (2020) 158–166. https://doi.org/10.1016/j.coche.2020.03.004.

[108] R.P. Rimington, A.J. Capel, S.D.R. Christie, M.P. Lewis, Biocompatible 3D printed polymers: Via fused deposition modelling direct C2C12 cellular phenotype in vitro, Lab on a Chip. 17 (2017) 2982–2993. https://doi.org/10.1039/c7lc00577f.

[109] E. Nyberg, A. Rindone, A. Dorafshar, W.L. Grayson, Comparison of 3D-Printed Poly-ϵ-Caprolactone Scaffolds Functionalized with Tricalcium Phosphate, Hydroxyapatite, Bio-Oss, or Decellularized Bone Matrix, Tissue Engineering - Part A. (2017). https://doi.org/10.1089/ten.tea.2016.0418.

[110] V. Raeisdasteh Hokmabad, S. Davaran, A. Ramazani, R. Salehi, Design and fabrication of porous biodegradable scaffolds: a strategy for tissue engineering, Journal of Biomaterials Science, Polymer Edition. 28 (2017) 1797–1825. https://doi.org/10.1080/09205063.2017.1354674.

[111] X. Zhang, W. Fan, T. Liu, Fused deposition modeling 3D printing of polyamide-based composites and its applications, Composites Communications. 21 (2020) 100413. https://doi.org/10.1016/j.coco.2020.100413.

[112] J.A. Lewis, Direct ink writing of 3D functional materials, Advanced Functional Materials. 16 (2006) 2193–2204. https://doi.org/10.1002/adfm.200600434.

[113] X. Wan, L. Luo, Y. Liu, J. Leng, Direct Ink Writing Based 4D Printing of Materials and Their Applications, Advanced Science. 7 (2020) 1–29. https://doi.org/10.1002/advs.202001000.

[114] Z. Liu, M. Zhang, B. Bhandari, Y. Wang, 3D printing: Printing precision and application in food sector, Trends in Food Science and Technology. 69 (2017) 83–94. https://doi.org/10.1016/j.tifs.2017.08.018.

[115] L. Li, Q. Lin, M. Tang, A.J.E. Duncan, C. Ke, Advanced Polymer Designs for Direct-Ink-Write 3D Printing, Chemistry - A European Journal. 25 (2019) 10768–10781. https://doi.org/10.1002/chem.201900975.

1346 [116] Y. Jiang, J. Plog, A.L. Yarin, Y. Pan, Direct ink writing of surface-modified flax
1347 elastomer composites, Composites Part B: Engineering. 194 (2020) 108061.
1348 https://doi.org/10.1016/j.compositesb.2020.108061.

1349 [117] O.D. Yirmibesoglu, L.E. Simonsen, R. Manson, J. Davidson, K. Healy, Y. Menguc,
1350 T. Wallin, Multi-material direct ink writing of photocurable elastomeric foams,
1351 Communications Materials. 2 (2021). https://doi.org/10.1038/s43246-021-00186-3.

1352 [118] J.A. Lewis, J.E. Smay, J. Stuecker, J. Cesarano, Direct ink writing of three-
1353 dimensional ceramic structures, Journal of the American Ceramic Society. 89
1354 (2006) 3599–3609. https://doi.org/10.1111/j.1551-2916.2006.01382.x.

1355 [119] N.W.S. Pinargote, A. Smirnov, N. Peretyagin, A. Seleznev, P. Peretyagin, Direct
1356 ink writing technology (3d printing) of graphene-based ceramic nanocomposites:
1357 A review, Nanomaterials. 10 (2020) 1–48. https://doi.org/10.3390/nano10071300.

1358 [120] J. Li, C. Wu, P.K. Chu, M. Gelinsky, 3D printing of hydrogels: Rational design
1359 strategies and emerging biomedical applications, Materials Science and
1360 Engineering R: Reports. 140 (2020) 100543.
1361 https://doi.org/10.1016/j.mser.2020.100543.

1362 [121] V.C.F. Li, C.K. Dunn, Z. Zhang, Y. Deng, H.J. Qi, Direct Ink Write (DIW) 3D
1363 Printed Cellulose Nanocrystal Aerogel Structures, Scientific Reports. 7 (2017) 1–
1364 8. https://doi.org/10.1038/s41598-017-07771-y.

1365 [122] S. Tagliaferri, A. Panagiotopoulos, C. Mattevi, Direct ink writing of energy
1366 materials, Materials Advances (RSC). 2 (2021) 540–563.
1367 https://doi.org/10.1039/d0ma00753f.

1368 [123] V. Saggiomo, A.H. Velders, Simple 3D Printed Scaffold-Removal Method for the
1369 Fabrication of Intricate Microfluidic Devices, Advanced Science. 2 (2015).
1370 https://doi.org/10.1002/advs.201500125.

1371 [124] L.P. Bressan, T.M. Lima, G.D. da Silveira, J.A.F. da Silva, Low-cost and simple
1372 FDM-based 3D-printed microfluidic device for the synthesis of metallic core–

1373 shell nanoparticles, SN Applied Sciences. 2 (2020) 1–8.
1374 https://doi.org/10.1007/s42452-020-2768-2.

1375 [125] L.P. Bressan, J. Robles-Najar, C.B. Adamo, R.F. Quero, B.M.C. Costa, D.P. de
1376 Jesus, J.A.F. da Silva, 3D-printed microfluidic device for the synthesis of silver
1377 and gold nanoparticles, Microchemical Journal. 146 (2019) 1083–1089.
1378 https://doi.org/10.1016/j.microc.2019.02.043.

1379 [126] M. Zeraatkar, M.D. de Tullio, A. Pricci, F. Pignatelli, G. Percoco, Exploiting
1380 limitations of fused deposition modeling to enhance mixing in 3D printed
1381 microfluidic devices, Rapid Prototyping Journal. 27 (2021) 1850–1859.
1382 https://doi.org/10.1108/RPJ-03-2021-0051.

1383 [127] F. Li, N.P. Macdonald, R.M. Guijt, M.C. Breadmore, Using Printing Orientation
1384 for Tuning Fluidic Behavior in Microfluidic Chips Made by Fused Deposition
1385 Modeling 3D Printing, Analytical Chemistry. 89 (2017) 12805–12811.
1386 https://doi.org/10.1021/acs.analchem.7b03228.

1387 [128] F. Kotz, M. Mader, N. Dellen, P. Risch, A. Kick, D. Helmer, B.E. Rapp, Fused
1388 deposition modeling of microfluidic chips in polymethylmethacrylate,
1389 Micromachines (Basel). 11 (2020) 5–8. https://doi.org/10.3390/mi11090873.

1390 [129] L.P. Bressan, C.B. Adamo, R.F. Quero, D.P. de Jesus, J.A.F. da Silva, A simple
1391 procedure to produce FDM-based 3D-printed microfluidic devices with an
1392 integrated PMMA optical window, Analytical Methods. 11 (2019) 1014–1020.
1393 https://doi.org/10.1039/c8ay02092b.

1394 [130] G. Gaal, M. Mendes, T.P. de Almeida, M.H.O. Piazzetta, Â.L. Gobbi, A. Riul, V.
1395 Rodrigues, Simplified fabrication of integrated microfluidic devices using fused
1396 deposition modeling 3D printing, Sensors and Actuators, B: Chemical. 242 (2017)
1397 35–40. https://doi.org/10.1016/j.snb.2016.10.110.

1398 [131] V. Romanov, R. Samuel, M. Chaharlang, A.R. Jafek, A. Frost, B.K. Gale, FDM 3D
1399 Printing of High-Pressure, Heat-Resistant, Transparent Microfluidic Devices,

Analytical Chemistry. 90 (2018) 10450–10456. https://doi.org/10.1021/acs.analchem.8b02356.

[132] T. Ching, Y. Li, R. Karyappa, A. Ohno, Y.C. Toh, M. Hashimoto, Fabrication of integrated microfluidic devices by direct ink writing (DIW) 3D printing, Sensors and Actuators, B: Chemical. 297 (2019) 126609. https://doi.org/10.1016/j.snb.2019.05.086.

[133] M. Athanasiadis, A. Pak, D. Afanasenkau, I.R. Minev, Direct Writing of Elastic Fibers with Optical, Electrical, and Microfluidic Functionality, Advanced Materials Technologies. 4 (2019). https://doi.org/10.1002/admt.201800659.

[134] D. Hur, M.G. Say, S.E. Diltemiz, F. Duman, A. Ersöz, R. Say, 3D Micropatterned All-Flexible Microfluidic Platform for Microwave-Assisted Flow Organic Synthesis, Chempluschem. 83 (2018) 42–46. https://doi.org/10.1002/cplu.201700440.

[135] Y. Alvarez-Braña, J. Etxebarria-Elezgarai, L. Ruiz de Larrinaga-Vicente, F. Benito-Lopez, L. Basabe-Desmonts, Modular micropumps fabricated by 3D printed technologies for polymeric microfluidic device applications, Sensors and Actuators, B: Chemical. 342 (2021). https://doi.org/10.1016/j.snb.2021.129991.

[136] F. Li, N.P. Macdonald, R.M. Guijt, M.C. Breadmore, Increasing the functionalities of 3D printed microchemical devices by single material, multimaterial, and print-pause-print 3D printing, Lab on a Chip. 19 (2019) 35–49. https://doi.org/10.1039/c8lc00826d.

[137] M. Kuang, L. Wang, Y. Song, Controllable Printing Droplets for High-Resolution Patterns, Advanced Materials. 26 (2014) 6950–6958. https://doi.org/10.1002/adma.201305416.

[138] FacFox documents, PolyJet vs MultiJet Printing(MJP), (2019). https://facfox.com/docs/kb/polyjet-mjp-comparison (accessed August 11, 2021).

1426 [139] H. Gudapati, M. Dey, I. Ozbolat, A comprehensive review on droplet-based
1427 bioprinting: Past, present and future, Biomaterials. 102 (2016) 20–42.
1428 https://doi.org/10.1016/j.biomaterials.2016.06.012.

1429 [140] W.L. Ng, W.Y. Yeong, M.W. Naing, Polyvinylpyrrolidone-based bio-ink
1430 improves cell viability and homogeneity during drop-on-demand printing,
1431 Materials. 10 (2017). https://doi.org/10.3390/ma10020190.

1432 [141] Y. Guo, H.S. Patanwala, B. Bognet, A.W.K. Ma, Inkjet and inkjet-based 3D
1433 printing: Connecting fluid properties and printing performance, Rapid
1434 Prototyping Journal. 23 (2017) 562–576. https://doi.org/10.1108/RPJ-05-2016-0076.

1435 [142] B. Derby, Bioprinting: Inkjet printing proteins and hybrid cell-containing
1436 materials and structures, Journal of Materials Chemistry. 18 (2008) 5717–5721.
1437 https://doi.org/10.1039/b807560c.

1438 [143] E.M. Kritchman, I. Zeytoun, RAPID PROTOTYPINGAPPARATUS (US 8.323.017
1439 B2), 2011.

1440 [144] Y. Yagci, S. Jockusch, N.J. Turro, Photoinitiated polymerization: Advances,
1441 challenges, and opportunities, Macromolecules. 43 (2010) 6245–6260.
1442 https://doi.org/10.1021/ma1007545.

1443 [145] J. V Crivello, E. Reichmanis, Photopolymer Materials and Processes for Advanced
1444 Technologies, (2014).

1445 [146] M. Gastaldi, F. Cardano, M. Zanetti, G. Viscardi, C. Barolo, S. Bordiga, S.
1446 Magdassi, A. Fin, I. Roppolo, Functional Dyes in Polymeric 3D Printing:
1447 Applications and Perspectives, (2021).
1448 https://doi.org/10.1021/acsmaterialslett.0c00455.

1449 [147] F. Wang, Y. Chong, F.K. Wang, C. He, Photopolymer resins for luminescent three-
1450 dimensional printing, Journal of Applied Polymer Science. 134 (2017) 1–8.
1451 https://doi.org/10.1002/app.44988.

1452 [148] M. Schuster, C. Turecek, B. Kaiser, J. Stampfl, R. Liska, F. Varga, Evaluation of
1453 biocompatible photopolymers I: Photoreactivity and mechanical properties of
1454 reactive diluents, Journal of Macromolecular Science, Part A: Pure and Applied
1455 Chemistry. 44 (2007) 547–557. https://doi.org/10.1080/10601320701235958.

1456 [149] M. Sugavaneswaran, G. Arumaikkannu, Analytical and experimental
1457 investigation on elastic modulus of reinforced additive manufactured structure,
1458 Materials and Design. 66 (2015) 29–36.
1459 https://doi.org/10.1016/j.matdes.2014.10.029.

1460 [150] N. Vidakis, M. Petousis, N. Vaxevanidis, J. Kechagias, Surface Roughness
1461 Investigation of Poly-Jet 3D Printing, Mathematics. 8 (2020) 1758.
1462 https://doi.org/10.3390/math8101758.

1463 [151] J.M. Lee, M. Zhang, W.Y. Yeong, Characterization and evaluation of 3D printed
1464 microfluidic chip for cell processing, Microfluidics and Nanofluidics. 20 (2016) 1–
1465 15. https://doi.org/10.1007/s10404-015-1688-8.

1466 [152] N.F. Ayub, S. Hashim, J. Jamaluddin, N. Adrus, New UV LED curing approach
1467 for polyacrylamide and poly(: N -isopropylacrylamide) hydrogels, New Journal
1468 of Chemistry. (2017). https://doi.org/10.1039/c7nj00176b.

1469 [153] V. Mucci, C. Vallo, Efficiency of 2,2-dimethoxy-2-phenylacetophenone for the
1470 photopolymerization of methacrylate monomers in thick sections, Journal of
1471 Applied Polymer Science. (2012). https://doi.org/10.1002/app.34473.

1472 [154] B. Steyrer, P. Neubauer, R. Liska, J. Stampfl, Visible light photoinitiator for 3D-
1473 printing of tough methacrylate resins, Materials. 10 (2017) 1–11.
1474 https://doi.org/10.3390/ma10121445.

1475 [155] H.K. Park, M. Shin, B. Kim, J.W. Park, H. Lee, A visible light-curable yet visible
1476 wavelength-transparent resin for stereolithography 3D printing, NPG Asia
1477 Materials. 10 (2018) 82–89. https://doi.org/10.1038/s41427-018-0021-x.

1478 [156] B.D. Fairbanks, M.P. Schwartz, C.N. Bowman, K.S. Anseth, Photoinitiated
1479 polymerization of PEG-diacrylate with lithium phenyl-2,4,6-
1480 trimethylbenzoylphosphinate: polymerization rate and cytocompatibility,
1481 Biomaterials. 30 (2009) 6702–6707.
1482 https://doi.org/10.1016/j.biomaterials.2009.08.055.

1483 [157] K. Wang, K. Yang, Q. Yu, Novel polymeric photoinitiators with side-chain
1484 benzophenone: Facile synthesis and photopolymerization properties without
1485 coinitiator, Progress in Organic Coatings. (2014).
1486 https://doi.org/10.1016/j.porgcoat.2014.06.026.

1487 [158] H. Matsushima, S. Hait, Q. Li, H. Zhou, M. Shirai, C.E. Hoyle, Non-extractable
1488 photoinitiators based on thiol-functionalized benzophenones and thioxanthones,
1489 European Polymer Journal. (2010).
1490 https://doi.org/10.1016/j.eurpolymj.2010.03.003.

1491 [159] Y.C. Chen, J.L. Ferracane, S.A. Prahl, Quantum yield of conversion of the
1492 photoinitiator camphorquinone, Dental Materials. (2007).
1493 https://doi.org/10.1016/j.dental.2006.06.005.

1494 [160] R.D. Sochol, E. Sweet, C.C. Glick, S. Venkatesh, A. Avetisyan, K.F. Ekman, A.
1495 Raulinaitis, A. Tsai, A. Wienkers, K. Korner, K. Hanson, A. Long, B.J. Hightower,
1496 G. Slatton, D.C. Burnett, T.L. Massey, K. Iwai, L.P. Lee, K.S.J. Pister, L. Lin, 3D
1497 printed microfluidic circuitry via multijet-based additive manufacturing, Lab on
1498 a Chip. 16 (2016) 668–678. https://doi.org/10.1039/c5lc01389e.

1499 [161] E. Sweet, R. Mehta, Y. Xu, R. Jew, R. Lin, L. Lin, Finger-powered fluidic actuation
1500 and mixing: Via MultiJet 3D printing, Lab on a Chip. 20 (2020) 3375–3385.
1501 https://doi.org/10.1039/d0lc00488j.

1502 [162] R. Walczak, K. Adamski, W. Kubicki, Inkjet 3D printed chip for capillary gel
1503 electrophoresis, Sensors and Actuators, B: Chemical. 261 (2018) 474–480.
1504 https://doi.org/10.1016/j.snb.2018.01.174.

1505 [163] E.A. Mansur, M. YE, Y. WANG, Y. DAI, A State-of-the-Art Review of Mixing in
1506 Microfluidic Mixers, Chinese Journal of Chemical Engineering. (2008).
1507 https://doi.org/10.1016/S1004-9541(08)60114-7.

1508 [164] C.Y. Lee, C.L. Chang, Y.N. Wang, L.M. Fu, Microfluidic mixing: A review,
1509 International Journal of Molecular Sciences. (2011).
1510 https://doi.org/10.3390/ijms12053263.

1511 [165] C.Y. Lee, W.T. Wang, C.C. Liu, L.M. Fu, Passive mixers in microfluidic systems:
1512 A review, Chemical Engineering Journal. (2016).
1513 https://doi.org/10.1016/j.cej.2015.10.122.

1514 [166] A. Enders, I.G. Siller, K. Urmann, M.R. Hoffmann, J. Bahnemann, 3D Printed
1515 Microfluidic Mixers—A Comparative Study on Mixing Unit Performances, Small.
1516 15 (2019) 1–9. https://doi.org/10.1002/smll.201804326.

1517 [167] C. Chen, B.T. Mehl, A.S. Munshi, A.D. Townsend, D.M. Spence, R.S. Martin, 3D-
1518 printed microfluidic devices: fabrication, advantages and limitations - a mini
1519 review, Analytical Methods. (2016). https://doi.org/10.1039/c6ay01671e.

1520 [168] A.M. Tothill, M. Partridge, S.W. James, R.P. Tatam, Fabrication and optimisation
1521 of a fused filament 3D-printed microfluidic platform, Journal of Micromechanics
1522 and Microengineering. 27 (2017). https://doi.org/10.1088/1361-6439/aa5ae3.

1523 [169] S.J. Keating, M.I. Gariboldi, W.G. Patrick, S. Sharma, D.S. Kong, N. Oxman, 3D
1524 printed multimaterial microfluidic valve, PLoS ONE. 11 (2016) 1–12.
1525 https://doi.org/10.1371/journal.pone.0160624.

1526 [170] W.L. Ng, J.M. Lee, M. Zhou, Y.W. Chen, K.X.A. Lee, W.Y. Yeong, Y.F. Shen, Vat
1527 polymerization-based bioprinting - process, materials, applications and
1528 regulatory challenges, Biofabrication. 12 (2020). https://doi.org/10.1088/1758-
1529 5090/ab6034.

1530 [171] W. Li, L.S. Mille, J.A. Robledo, T. Uribe, V. Huerta, Y.S. Zhang, Recent Advances
1531 in Formulating and Processing Biomaterial Inks for Vat Polymerization-Based 3D

1532 Printing, Advanced Healthcare Materials. 9 (2020) 1–18.
1533 https://doi.org/10.1002/adhm.202000156.

1534 [172] F.P.W. Melchels, J. Feijen, D.W. Grijpma, A review on stereolithography and its
1535 applications in biomedical engineering, Biomaterials. 31 (2010) 6121–6130.
1536 https://doi.org/10.1016/j.biomaterials.2010.04.050.

1537 [173] R.D. Farahani, M. Dubé, D. Therriault, Three-Dimensional Printing of
1538 Multifunctional Nanocomposites: Manufacturing Techniques and Applications,
1539 Advanced Materials. (2016) 5794–5821. https://doi.org/10.1002/adma.201506215.

1540 [174] M.G. Guerra, C. Volpone, L.M. Galantucci, G. Percoco, Photogrammetric
1541 measurements of 3D printed microfluidic devices, Additive Manufacturing. 21
1542 (2018) 53–62. https://doi.org/10.1016/j.addma.2018.02.013.

1543 [175] H. Kodama, Automatic method for fabricating a three-dimensional plastic model
1544 with photo-hardening polymer, Review of Scientific Instruments. (1981).
1545 https://doi.org/10.1063/1.1136492.

1546 [176] C.W. Hull, Apparatus for Production of Three-Dimensonal Objects By
1547 Stereolithography, Patent. (1984) 16.

1548 [177] A. Oesterreicher, J. Wiener, M. Roth, A. Moser, R. Gmeiner, M. Edler, G. Pinter,
1549 T. Griesser, Tough and degradable photopolymers derived from alkyne
1550 monomers for 3D printing of biomedical materials, Polymer Chemistry. (2016).
1551 https://doi.org/10.1039/c6py01132b.

1552 [178] K. Ikuta, K. Hirowatari, Real three dimensional micro fabrication using stereo
1553 lithography and metal molding, in: Proceedings IEEE Micro Electro Mechanical
1554 Systems, Fort Lauderdale, FL, USA, 1993: pp. 42–27.
1555 https://doi.org/10.1109/MEMSYS.1993.296949.

1556 [179] J. DeSimone, E. Sarnulski, A. Ermoshkin, P. DeSimone, Rapid 3D Continuous
1557 Printing of Casting Molds for Metals and Other Materials, WO 2015/080888A2,
1558 2015.

1559 [180] H. Quan, T. Zhang, H. Xu, S. Luo, J. Nie, X. Zhu, Photo-curing 3D printing
1560 technique and its challenges, Bioactive Materials. (2020).
1561 https://doi.org/10.1016/j.bioactmat.2019.12.003.

1562 [181] J.F. Xing, M.L. Zheng, X.M. Duan, Two-photon polymerization microfabrication
1563 of hydrogels: an advanced 3D printing technology for tissue engineering and
1564 drug delivery, Chemical Society Reviews. (2015).
1565 https://doi.org/10.1039/c5cs00278h.

1566 [182] I. Bhattacharya, B. Kelly, M. Shusteff, C. Spadaccini, H. Taylor, Computed axial
1567 lithography: volumetric 3D printing of arbitrary geometries (Conference
1568 Presentation), in: 2018. https://doi.org/10.1117/12.2307780.

1569 [183] H. Li, W. Fan, X. Zhu, Three-dimensional printing: The potential technology
1570 widely used in medical fields, Journal of Biomedical Materials Research - Part A.
1571 (2020). https://doi.org/10.1002/jbm.a.36979.

1572 [184] P. Juskova, A. Ollitrault, M. Serra, J.L. Viovy, L. Malaquin, Resolution
1573 improvement of 3D stereo-lithography through the direct laser trajectory
1574 programming: Application to microfluidic deterministic lateral displacement
1575 device, Analytica Chimica Acta. (2018). https://doi.org/10.1016/j.aca.2017.11.062.

1576 [185] Y. Liu, Q. Hu, F. Zhang, C. Tuck, D. Irvine, R. Hague, Y. He, M. Simonelli, G.A.
1577 Rance, E.F. Smith, R.D. Wildman, Additive manufacture of three dimensional
1578 nanocomposite based objects through multiphoton fabrication, Polymers (Basel).
1579 8 (2016) 325. https://doi.org/10.3390/polym8090325.

1580 [186] Y.-L. Cheng, H.-L. Kao, Study on visible-light-curable polycarprolactone and
1581 poly(ethylene glycol) diacrylate for LCD-projected maskless additive
1582 manufacturing system, in: Light Manipulating Organic Materials and Devices II,
1583 2015. https://doi.org/10.1117/12.2188047.

1584 [187] S.H. Kim, Y.K. Yeon, J.M. Lee, J.R. Chao, Y.J. Lee, Y.B. Seo, M.T. Sultan, O.J. Lee,
1585 J.S. Lee, S. Il Yoon, I.S. Hong, G. Khang, S.J. Lee, J.J. Yoo, C.H. Park, Precisely

1586 printable and biocompatible silk fibroin bioink for digital light processing 3D
1587 printing, Nature Communications. 9 (2018) 1–14. https://doi.org/10.1038/s41467-
1588 018-03759-y.

1589 [188] C. Yu, J. Schimelman, P. Wang, K.L. Miller, X. Ma, S. You, J. Guan, B. Sun, W.
1590 Zhu, S. Chen, Photopolymerizable Biomaterials and Light-Based 3D Printing
1591 Strategies for Biomedical Applications, Chemical Reviews. (2020).
1592 https://doi.org/10.1021/acs.chemrev.9b00810.

1593 [189] A.K. Nguyen, R.J. Narayan, Two-photon polymerization for biological
1594 applications, Materials Today. (2017).
1595 https://doi.org/10.1016/j.mattod.2017.06.004.

1596 [190] R. Infuehr, J. Stampfl, S. Krivec, R. Liska, H. Lichtenegger, V. Satzinger, V.
1597 Schmidt, N. Matsko, W. Grogger, 3D-structuring of optical waveguides with two
1598 photon polymerization, MRS Proceedings. 1179 (2009) 1179-BB01-07.
1599 https://doi.org/10.1557/PROC-1179-BB01-07.

1600 [191] R. Whitby, Y. Ben-Tal, R. MacMillan, S. Janssens, S. Raymond, D. Clarke, J. Jin, A.
1601 Kay, M.C. Simpson, Photoinitiators for two-photon polymerisation: effect of
1602 branching and viscosity on polymerisation thresholds, RSC Advances. 7 (2017)
1603 13232–13239. https://doi.org/10.1039/c6ra27176f.

1604 [192] B.E. Kelly, I. Bhattacharya, H. Heidari, M. Shusteff, C.M. Spadaccini, H.K. Taylor,
1605 Volumetric additive manufacturing via tomographic reconstruction, Science
1606 (1979). (2019). https://doi.org/10.1126/science.aau7114.

1607 [193] B.E. Kelly, I. Bhattacharya, M. Shusteff, H.K. Taylor, C.M. Spaddacini, Computed
1608 axial lithography for rapid volumetric 3D additive manufacturing, in: Solid
1609 Freeform Fabrication 2017: Proceedings of the 28th Annual International Solid
1610 Freeform Fabrication Symposium - An Additive Manufacturing Conference, SFF
1611 2017, 2020.

1612 [194] P.N. Bernal, P. Delrot, D. Loterie, Y. Li, J. Malda, C. Moser, R. Levato,
1613 Biofabrication: Volumetric Bioprinting of Complex Living-Tissue Constructs
1614 within Seconds (Adv. Mater. 42/2019), Advanced Materials. (2019).
1615 https://doi.org/10.1002/adma.201970302.

1616 [195] J.P. Fouassier, J. Lalevée, Photoinitiators for Polymer Synthesis, 2012.
1617 https://doi.org/10.1002/9783527648245.

1618 [196] B. Narupai, A. Nelson, 100th Anniversary of Macromolecular Science Viewpoint:
1619 Macromolecular Materials for Additive Manufacturing, ACS Macro Letters.
1620 (2020) 627–638. https://doi.org/10.1021/acsmacrolett.0c00200.

1621 [197] J. Lammel-Lindemann, I.A. Dourado, J. Shanklin, C.A. Rodriguez, L.H. Catalani,
1622 D. Dean, Photocrosslinking-based 3D printing of unsaturated polyesters from
1623 isosorbide: A new material for resorbable medical devices, Bioprinting. (2020).
1624 https://doi.org/10.1016/j.bprint.2019.e00062.

1625 [198] P.J. Scott, V. Meenakshisundaram, M. Hegde, C.R. Kasprzak, C.R. Winkler, K.D.
1626 Feller, C.B. Williams, T.E. Long, 3D Printing Latex: A Route to Complex
1627 Geometries of High Molecular Weight Polymers, ACS Applied Materials and
1628 Interfaces. (2020). https://doi.org/10.1021/acsami.9b19986.

1629 [199] H. Leonards, S. Engelhardt, A. Hoffmann, L. Pongratz, S. Schriever, J. Bläsius, M.
1630 Wehner, A. Gillner, Advantages and drawbacks of Thiol-ene based resins for 3D-
1631 printing, in: Laser 3D Manufacturing II, 2015. https://doi.org/10.1117/12.2081169.

1632 [200] T. Zhao, X. Li, R. Yu, Y. Zhang, X. Yang, X. Zhao, L. Wang, W. Huang, Silicone–
1633 Epoxy-Based Hybrid Photopolymers for 3D Printing, Macromolecular Chemistry
1634 and Physics. 219 (2018) 1–10. https://doi.org/10.1002/macp.201700530.

1635 [201] A. Bagheri, J. Jin, Photopolymerization in 3D Printing, ACS Applied Polymer
1636 Materials. 1 (2019) 593–611. https://doi.org/10.1021/acsapm.8b00165.

1637 [202] S. Shanmugam, J. Xu, C. Boyer, Light-regulated polymerization under near-
1638 infrared/far-red irradiation catalyzed by bacteriochlorophyll a, Angewandte
1639 Chemie - International Edition. (2016). https://doi.org/10.1002/anie.201510037.

1640 [203] N. Corrigan, J. Xu, C. Boyer, A Photoinitiation System for Conventional and
1641 Controlled Radical Polymerization at Visible and NIR Wavelengths,
1642 Macromolecules. (2016). https://doi.org/10.1021/acs.macromol.6b00542.

1643 [204] A. Al Mousawi, C. Poriel, F. Dumur, J. Toufaily, T. Hamieh, J.P. Fouassier, J.
1644 Lalevée, Zinc Tetraphenylporphyrin as High Performance Visible Light
1645 Photoinitiator of Cationic Photosensitive Resins for LED Projector 3D Printing
1646 Applications, Macromolecules. (2017).
1647 https://doi.org/10.1021/acs.macromol.6b02596.

1648 [205] J. Xu, S. Shanmugam, C. Fu, K.F. Aguey-Zinsou, C. Boyer, Selective
1649 Photoactivation: From a Single Unit Monomer Insertion Reaction to Controlled
1650 Polymer Architectures, J Am Chem Soc. (2016).
1651 https://doi.org/10.1021/jacs.5b12408.

1652 [206] B.M. Hong, S.A. Park, W.H. Park, Effect of photoinitiator on chain degradation of
1653 hyaluronic acid, Biomaterials Research. (2019). https://doi.org/10.1186/s40824-
1654 019-0170-1.

1655 [207] J. Zhang, J. Lalevée, J. Zhao, B. Graff, M.H. Stenzel, P. Xiao,
1656 Dihydroxyanthraquinone derivatives: Natural dyes as blue-light-sensitive
1657 versatile photoinitiators of photopolymerization, Polymer Chemistry. (2016).
1658 https://doi.org/10.1039/c6py01550f.

1659 [208] F. Masson, C. Decker, S. Andre, X. Andrieu, UV-curable formulations for UV-
1660 transparent optical fiber coatings: I. Acrylic resins, Progress in Organic Coatings.
1661 49 (2004) 1–12. https://doi.org/10.1016/S0300-9440(03)00122-X.

1662 [209] J.P. Fouassier, J. Lalevée, Photoinitiators for Polymer Synthesis, 2012.
1663 https://doi.org/10.1002/9783527648245.

1664 [210] M. Stemmelen, F. Pessel, V. Lapinte, S. Caillol, J.P. Habas, J.J. Robin, A fully
1665 biobased epoxy resin from vegetable oils: From the synthesis of the precursors by
1666 thiol-ene reaction to the study of the final material, Journal of Polymer Science,
1667 Part A: Polymer Chemistry. 49 (2011) 2434–2444.
1668 https://doi.org/10.1002/pola.24674.

1669 [211] A. Ravve, Light-Associated Reactions of Synthetic Polymers, Springer US, 2006.

1670 [212] A. Santini, I.T. Gallegos, C.M. Felix, Photoinitiators in dentistry: a review., Prim
1671 Dent J. (2013). https://doi.org/10.1308/205016814809859563.

1672 [213] I. Kunio, E. Takeshi, A review of the development of radical photopolymerization
1673 initiators used for designing light-curing dental adhesives and resin composites,
1674 Dental Materials Journal. (2010). https://doi.org/10.4012/dmj.2009-137.

1675 [214] J. Lalevée, F. Morlet-Savary, C. Dietlin, B. Graff, J.P. Fouassier, Photochemistry
1676 and radical chemistry under low intensity visible light sources: Application to
1677 photopolymerization reactions, Molecules. (2014).
1678 https://doi.org/10.3390/molecules190915026.

1679 [215] M. Kaur, A.K. Srivastava, Photopolymerization: A review, Journal of
1680 Macromolecular Science - Polymer Reviews. (2002). https://doi.org/10.1081/MC-
1681 120015988.

1682 [216] C. Kutall, P.A. Grutsch, D.B. Yang, A novel strategy for photoinitiated anionic-
1683 polymerization, Macromolecules. 24 (1991) 6872–6873.
1684 https://doi.org/10.1021/ma00026a016.

1685 [217] B.J. Palmer, C. Kutal, R. Billing, H. Hening, A new photoinitiator for anionic-
1686 polymerization, Macromolecules. 28 (1995) 1328–1329.
1687 https://doi.org/10.1021/ma00108a078.

1688 [218] Y.H. Wang, P. Wan, Ketoprofen as a photoinitiator for anionic polymerization,
1689 Photochemical and Photobiological Sciences. (2015).
1690 https://doi.org/10.1039/c4pp00454j.

1691 [219] M. Rahal, H. Mokbel, B. Gra, J. Toufaily, T. Hamieh, J. Lalev, Mono vs.
1692 Difunctional Coumarin as Photoinitiators in Photocomposite Synthesis and 3D
1693 Printing, Catalysts. 10 (2020) 1–18. https://doi.org/doi:10.3390/catal10101202.

1694 [220] A.K. Nguyen, P.L. Goering, R.K. Elespuru, S.S. Das, R.J. Narayan, The
1695 photoinitiator lithium phenyl (2,4,6-Trimethylbenzoyl) phosphinate with
1696 exposure to 405 nm light is cytotoxic to mammalian cells but not mutagenic in
1697 bacterial reverse mutation assays, Polymers (Basel). 12 (2020) 1–13.
1698 https://doi.org/10.3390/polym12071489.

1699 [221] W. Tomal, J. Ortyl, Water-soluble photoinitiators in biomedical applications,
1700 Polymers (Basel). 12 (2020) 1–30. https://doi.org/10.3390/POLYM12051073.

1701 [222] T.N. Eren, T. Gencoglu, M. Abdallah, J. Lalevée, D. Avci, A water soluble and
1702 highly reactive bisphosphonate functionalized thioxanthone-based
1703 photoinitiator, European Polymer Journal. 135 (2020) 109906.
1704 https://doi.org/10.1016/j.eurpolymj.2020.109906.

1705 [223] L. Breloy, C. Negrell, A.S. Mora, W.S.J. Li, V. Brezová, S. Caillol, D.L. Versace,
1706 Vanillin derivative as performing type I photoinitiator, European Polymer
1707 Journal. 132 (2020) 109727. https://doi.org/10.1016/j.eurpolymj.2020.109727.

1708 [224] D.M. Love, B.D. Fairbanks, C.N. Bowman, Evaluation of Aromatic Thiols as
1709 Photoinitiators, Macromolecules. 53 (2020) 5237–5247.
1710 https://doi.org/10.1021/acs.macromol.0c00757.

1711 [225] S. Liu, H. Chen, Y. Zhang, K. Sun, Y. Xu, F. Morlet-Savary, B. Graff, G. Noirbent,
1712 C. Pigot, D. Brunel, M. Nechab, D. Gigmes, P. Xiao, F. Dumur, J. Lalevée,
1713 Monocomponent photoinitiators based on benzophenone-carbazole structure for
1714 LED photoinitiating systems and application on 3D printing, Polymers (Basel). 12
1715 (2020) 1–15. https://doi.org/10.3390/polym12061394.

1716 [226] R. Ni, B. Qian, C. Liu, X. Liu, J. Qiu, Three-dimensional printing of hybrid
1717 organic/inorganic composites with long persistence luminescence, Optical

Materials Express. 8 (2018) 2823–2831. https://doi.org/10.1016/S0920-9964(12)70638-2.

[227] J. Palaganas, A.C. de Leon, J. Mangadlao, N. Palaganas, A. Mael, Y.J. Lee, H.Y. Lai, R. Advincula, Facile Preparation of Photocurable Siloxane Composite for 3D Printing, Macromolecular Materials and Engineering. 302 (2017) 1–9. https://doi.org/10.1002/mame.201600477.

[228] C.M. González-Henríquez, G. del C. Pizarro, M.A. Sarabia-Vallejos, C.A. Terraza, Z.E. López-Cabaña, In situ-preparation and characterization of silver-HEMA/PEGDA hydrogel matrix nanocomposites: Silver inclusion studies into hydrogel matrix, Arabian Journal of Chemistry. (2014). https://doi.org/10.1016/j.arabjc.2014.11.012.

[229] E.T. Tenório-Neto, M.R. Guilherme, M.E.G. Winkler, L. Cardozo-Filho, S.C. Beneti, A.F. Rubira, M.H. Kunita, Synthesis and characterization of silver nanoparticle nanocomposite thin films with thermally induced surface morphology changes, Materials Letters. 159 (2015) 118–121. https://doi.org/10.1016/j.matlet.2015.06.095.

[230] V. Jankauskaite, A. Lazauskas, E. Gri Konis, A. Lisauskaite, K. Ukiene, UV-curable aliphatic silicone acrylate organic–inorganic hybrid coatings with antibacterial activity, Molecules. 22 (2017). https://doi.org/10.3390/molecules22060964.

[231] Y.-C. Chen, T.-Y. Liu, Y.-H. Li, Photoreactivity study of photoinitiated free radical polymerization using Type II photoinitiator containing thioxanthone initiator as a hydrogen acceptor and various amine-type co-initiators as hydrogen donors, Journal of Coatings Technology and Research. (2020). https://doi.org/10.1007/s11998-020-00401-9.

[232] G. Gonzalez, A. Chiappone, I. Roppolo, E. Fantino, V. Bertana, F. Perrucci, L. Scaltrito, F. Pirri, M. Sangermano, Development of 3D printable formulations

1745 containing CNT with enhanced electrical properties, Polymer (Guildf). 109 (2016)
1746 246–253. https://doi.org/10.1016/j.polymer.2016.12.051.

1747 [233] J.S. Manzano, Z.B. Weinstein, A.D. Sadow, I.I. Slowing, Direct 3D Printing of
1748 Catalytically Active Structures, ACS Catalysis. 7 (2017) 7567–7577.
1749 https://doi.org/10.1021/acscatal.7b02111.

1750 [234] G.A. González Flores, V. Bertana, A. Chiappone, I. Roppolo, L. Scaltrito, S.L.
1751 Marasso, M. Cocuzza, G. Massaglia, M. Quaglio, C.F. Pirri, S. Ferrero, Single-Step
1752 3D Printing of Silver-Patterned Polymeric Devices for Bacteria Proliferation
1753 Control, Macromolecular Materials and Engineering. 2100596 (2021) 2100596.
1754 https://doi.org/10.1002/mame.202100596.

1755 [235] P.F. Costa, H.J. Albers, J.E.A. Linssen, H.H.T. Middelkamp, L. Van Der Hout, R.
1756 Passier, A. Van Den Berg, J. Malda, A.D. Van Der Meer, Mimicking arterial
1757 thrombosis in a 3D-printed microfluidic: In vitro vascular model based on
1758 computed tomography angiography data, Lab on a Chip. 17 (2017) 2785–2792.
1759 https://doi.org/10.1039/c7lc00202e.

1760 [236] P. Heo, S. Ramakrishnan, J. Coleman, J.E. Rothman, J.B. Fleury, F. Pincet, Highly
1761 Reproducible Physiological Asymmetric Membrane with Freely Diffusing
1762 Embedded Proteins in a 3D-Printed Microfluidic Setup, Small. 15 (2019) 1–13.
1763 https://doi.org/10.1002/smll.201900725.

1764 [237] C.L. Manzanares Palenzuela, M. Pumera, (Bio)Analytical chemistry enabled by
1765 3D printing: Sensors and biosensors, TrAC - Trends in Analytical Chemistry. 103
1766 (2018) 110–118. https://doi.org/10.1016/j.trac.2018.03.016.

1767 [238] D.J. Wales, Q. Cao, K. Kastner, E. Karjalainen, G.N. Newton, V. Sans, 3D-Printable
1768 Photochromic Molecular Materials for Reversible Information Storage, Advanced
1769 Materials. 30 (2018) 1–7. https://doi.org/10.1002/adma.201800159.

1770 [239] A.K. Au, W. Lee, A. Folch, Mail-order microfluidics: Evaluation of
1771 stereolithography for the production of microfluidic devices, Lab on a Chip. 14
1772 (2014) 1294–1301. https://doi.org/10.1039/c3lc51360b.

1773 [240] A.I. Shallan, P. Smejkal, M. Corban, R.M. Guijt, M.C. Breadmore, Cost-effective
1774 three-dimensional printing of visibly transparent microchips within minutes,
1775 Analytical Chemistry. 86 (2014) 3124–3130. https://doi.org/10.1021/ac4041857.

1776 [241] H. Gong, M. Beauchamp, S. Perry, A. Woolley, G. Nordin, Optical Approach to
1777 Resin Formulation for 3D Printed Microfluidics, RSC Advances. 5 (2015) 106621–
1778 106632. https://doi.org/10.1039/C5RA23855B.

1779 [242] M.J. Beauchamp, H. Gong, A.T. Woolley, G.P. Nordin, 3D printed microfluidic
1780 features using dose control in X, Y, and Z dimensions, Micromachines (Basel). 9
1781 (2018). https://doi.org/10.3390/mi9070326.

1782 [243] E.K. Parker, A. V. Nielsen, M.J. Beauchamp, H.M. Almughamsi, J.B. Nielsen, M.
1783 Sonker, H. Gong, G.P. Nordin, A.T. Woolley, 3D printed microfluidic devices
1784 with immunoaffinity monoliths for extraction of preterm birth biomarkers,
1785 Analytical and Bioanalytical Chemistry. 411 (2019) 5405–5413.
1786 https://doi.org/10.1007/s00216-018-1440-9.

1787 [244] M.J. Beauchamp, A. V. Nielsen, H. Gong, G.P. Nordin, A.T. Woolley, 3D Printed
1788 Microfluidic Devices for Microchip Electrophoresis of Preterm Birth Biomarkers,
1789 Analytical Chemistry. 91 (2019) 7418–7425.
1790 https://doi.org/10.1021/acs.analchem.9b01395.

1791 [245] M.J. Männel, L. Selzer, R. Bernhardt, J. Thiele, Optimizing Process Parameters in
1792 Commercial Micro-Stereolithography for Forming Emulsions and Polymer
1793 Microparticles in Nonplanar Microfluidic Devices, Advanced Materials
1794 Technologies. 4 (2019) 1–10. https://doi.org/10.1002/admt.201800408.

1795 [246] C. Yeung, S. Chen, B. King, H. Lin, K. King, F. Akhtar, G. Diaz, B. Wang, J. Zhu,
1796 W. Sun, A. Khademhosseini, S. Emaminejad, A 3D-printed microfluidic-enabled

1797 hollow microneedle architecture for transdermal drug delivery, Biomicrofluidics.
1798 13 (2019). https://doi.org/10.1063/1.5127778.

1799 [247] N. Bhattacharjee, C. Parra-Cabrera, Y.T. Kim, A.P. Kuo, A. Folch, Desktop-
1800 Stereolithography 3D-Printing of a Poly(dimethylsiloxane)-Based Material with
1801 Sylgard-184 Properties, Advanced Materials. 30 (2018) 1–7.
1802 https://doi.org/10.1002/adma.201800001.

1803 [248] F. Kotz, P. Risch, D. Helmer, B.E. Rapp, Highly fluorinated methacrylates for
1804 optical 3D printing of microfluidic devices, Micromachines (Basel). 9 (2018).
1805 https://doi.org/10.3390/mi9030115.

1806 [249] C.I. Rogers, K. Qaderi, A.T. Woolley, G.P. Nordin, 3D printed microfluidic
1807 devices with integrated valves, Biomicrofluidics. 9 (2015) 1–9.
1808 https://doi.org/10.1063/1.4905840.

1809 [250] H. Gong, A.T. Woolley, G.P. Nordin, High density 3D printed microfluidic
1810 valves, pumps, and multiplexers, Lab on a Chip. 16 (2016) 2450–2458.
1811 https://doi.org/10.1039/c6lc00565a.

1812 [251] J.L. Sanchez Noriega, N.A. Chartrand, J.C. Valdoz, C.G. Cribbs, D.A. Jacobs, D.
1813 Poulson, M.S. Viglione, A.T. Woolley, P.M. van Ry, K.A. Christensen, G.P.
1814 Nordin, Spatially and optically tailored 3D printing for highly miniaturized and
1815 integrated microfluidics, Nature Communications. 12 (2021).
1816 https://doi.org/10.1038/s41467-021-25788-w.

1817 [252] Y.S. Lee, N. Bhattacharjee, A. Folch, 3D-printed Quake-style microvalves and
1818 micropumps, Lab on a Chip. 18 (2018) 1207–1214.
1819 https://doi.org/10.1039/c8lc00001h.

1820 [253] S. Takenaga, B. Schneider, E. Erbay, M. Biselli, T. Schnitzler, M.J. Schöning, T.
1821 Wagner, Fabrication of biocompatible lab-on-chip devices for biomedical
1822 applications by means of a 3D-printing process, Physica Status Solidi (A)

1823 Applications and Materials Science. 212 (2015) 1347–1352.
1824 https://doi.org/10.1002/pssa.201532053.

1825 [254] A.P. Kuo, N. Bhattacharjee, Y.S. Lee, K. Castro, Y.T. Kim, A. Folch, High-Precision
1826 Stereolithography of Biomicrofluidic Devices, Advanced Materials Technologies.
1827 1800395 (2019) 1–11. https://doi.org/10.1002/admt.201800395.

1828 [255] Z. Wang, N. Martin, D. Hini, B. Mills, K. Kim, Rapid fabrication of multilayer
1829 microfluidic devices using the liquid crystal display-based stereolithography 3D
1830 printing system, 3D Printing and Additive Manufacturing. 4 (2017) 156–164.
1831 https://doi.org/10.1089/3dp.2017.0028.

1832 [256] S. Zips, L. Hiendlmeier, L.J.K. Weiß, H. Url, T.F. Teshima, R. Schmid, M.
1833 Eblenkamp, P. Mela, B. Wolfrum, Biocompatible, Flexible, and Oxygen-
1834 Permeable Silicone-Hydrogel Material for Stereolithographic Printing of
1835 Microfluidic Lab-On-A-Chip and Cell-Culture Devices, ACS Applied Polymer
1836 Materials. (2020). https://doi.org/10.1021/acsapm.0c01071.

1837 [257] G. Gonzalez, A. Chiappone, K. Dietliker, C.F. Pirri, I. Roppolo, Fabrication and
1838 Functionalization of 3D Printed Polydimethylsiloxane-Based Microfluidic
1839 Devices Obtained through Digital Light Processing, Advanced Materials
1840 Technologies. 5 (2020) 2000374. https://doi.org/10.1002/admt.202000374.

1841 [258] J. Berger, M.Y. Aydin, R. Stavins, J. Heredia, A. Mostafa, A. Ganguli, E. Valera, R.
1842 Bashir, W.P. King, Portable Pathogen Diagnostics Using Microfluidic Cartridges
1843 Made from Continuous Liquid Interface Production Additive Manufacturing,
1844 Analytical Chemistry. 93 (2021) 10048–10055.
1845 https://doi.org/10.1021/acs.analchem.1c00654.

1846 [259] Carbon3D, RPU 70, (2021). https://www.carbon3d.com/materials/rpu-70/
1847 (accessed August 21, 2021).

1848 [260] W. Wu, A. Deconinck, J.A. Lewis, Omnidirectional printing of 3D microvascular
1849 networks, Advanced Materials. 23 (2011) 178–183.
1850 https://doi.org/10.1002/adma.201004625.

1851 [261] K.S. Lim, J.H. Galarraga, X. Cui, G.C.J. Lindberg, J.A. Burdick, T.B.F. Woodfield,
1852 Fundamentals and Applications of Photo-Cross-Linking in Bioprinting, Chemical
1853 Reviews. (2020). https://doi.org/10.1021/acs.chemrev.9b00812.

1854 [262] J.Y. Lee, J. An, C.K. Chua, Fundamentals and applications of 3D printing for novel
1855 materials, Applied Materials Today. 7 (2017) 120–133.
1856 https://doi.org/10.1016/j.apmt.2017.02.004.

1857 [263] M. Layani, X. Wang, S. Magdassi, Novel Materials for 3D Printing by
1858 Photopolymerization, Advanced Materials. 30 (2018) 1–7.
1859 https://doi.org/10.1002/adma.201706344.

1860 [264] L.S. Andrews, J.J. Clary, Review of the toxicity of multifunctional acrylates,
1861 Journal of Toxicology and Environmental Health. (1986).
1862 https://doi.org/10.1080/15287398609530916.

1863 [265] F. Zhu, J. Skommer, T. Friedrich, J. Kaslin, D. Wlodkowic, 3D printed polymers
1864 toxicity profiling: A caution for biodevice applications, in: SPIE Micro+Nano
1865 Materials, Devices, and Applications Symposium, Sidney, Australia, n.d.
1866 https://doi.org/10.1117/12.2202392.

1867 [266] R. Zhang, N.B. Larsen, Stereolithographic hydrogel printing of 3D culture chips
1868 with biofunctionalized complex 3D perfusion networks, Lab on a Chip. 17 (2017)
1869 4273–4282. https://doi.org/10.1039/c7lc00926g.

1870 [267] A.D. Benjamin, R. Abbasi, M. Owens, R.J. Olsen, D.J. Walsh, T.B. Lefevre, J.N.
1871 Wilking, Light-based 3D printing of hydrogels with high-resolution channels,
1872 Biomedical Physics and Engineering Express. (2019).
1873 https://doi.org/10.1088/2057-1976/aad667.

1874 [268] A.A. Pawar, G. Saada, I. Cooperstein, L. Larush, J.A. Jackman, S.R. Tabaei, N.J.
1875 Cho, S. Magdassi, High-performance 3D printing of hydrogels by water-
1876 dispersible photoinitiator nanoparticles, Science Advances. 2 (2016).
1877 https://doi.org/10.1126/sciadv.1501381.

1878 [269] J.F. Xing, M.L. Zheng, X.M. Duan, Two-photon polymerization microfabrication
1879 of hydrogels: an advanced 3D printing technology for tissue engineering and
1880 drug delivery, Chemical Society Reviews. (2015).
1881 https://doi.org/10.1039/c5cs00278h.

1882 [270] Y. Zhang, D. An, Y. Pardo, A. Chiu, W. Song, Q. Liu, F. Zhou, S.P. McDonough,
1883 M. Ma, High-water-content and resilient PEG-containing hydrogels with low
1884 fibrotic response, Acta Biomaterialia. 53 (2017) 100–108.
1885 https://doi.org/10.1016/j.actbio.2017.02.028.

1886 [271] Y.S. Kim, K. Cho, H.J. Lee, S. Chang, H. Lee, J.H. Kim, W.G. Koh, Highly
1887 conductive and hydrated PEG-based hydrogels for the potential application of a
1888 tissue engineering scaffold, Reactive and Functional Polymers. 109 (2016) 15–22.
1889 https://doi.org/10.1016/j.reactfunctpolym.2016.09.003.

1890 [272] C.M. González-Henríquez, F.E. Rodriguez-Umanzor, J. Almagro-Correa, M.A.
1891 Sarabia-Vallejos, E. Martínez-Campos, M. Esteban-Lucía, A. del Campo-García, J.
1892 Rodríguez-Hernández, Biocompatible fluorinated wrinkled hydrogel films with
1893 antimicrobial activity, Materials Science and Engineering C. 114 (2020) 111031.
1894 https://doi.org/10.1016/j.msec.2020.111031.

1895 [273] M.J. Männel, C. Fischer, J. Thiele, A Non-Cytotoxic Resin for Micro-
1896 Stereolithography for Cell Cultures of HUVECs., Micromachines (Basel). 11
1897 (2020). https://doi.org/10.3390/mi11030246.

1898 [274] C. Warr, J.C. Valdoz, B.P. Bickham, C.J. Knight, N.A. Franks, N. Chartrand, P.M.
1899 Van Ry, K.A. Christensen, G.P. Nordin, A.D. Cook, Biocompatible PEGDA Resin

1900 for 3D Printing, ACS Applied Bio Materials. 3 (2020) 2239–2244.
1901 https://doi.org/10.1021/acsabm.0c00055.

1902 [275] MicronInc, FDA Approved 3D Printer Resins, (2017).
1903 https://www.microndental.com/regulatory/fda-approved-cleared-3d-printer-
1904 resins (accessed October 30, 2019).

1905 [276] K. Piironen, M. Haapala, V. Talman, P. Järvinen, T. Sikanen, Cell adhesion and
1906 proliferation on common 3D printing materials used in stereolithography of
1907 microfluidic devices, Lab on a Chip. 20 (2020) 2372–2382.
1908 https://doi.org/10.1039/d0lc00114g.

1909 [277] S. Kreß, R. Schaller-Ammann, J. Feiel, J. Priedl, C. Kasper, D. Egger, 3D printing
1910 of cell culture devices: Assessment and prevention of the cytotoxicity of
1911 photopolymers for stereolithography, Materials. 13 (2020).
1912 https://doi.org/10.3390/ma13133011.

1913 [278] R.P. Rimington, A.J. Capel, D.J. Player, R.J. Bibb, S.D.R. Christie, M.P. Lewis,
1914 Feasibility and Biocompatibility of 3D-Printed Photopolymerized and Laser
1915 Sintered Polymers for Neuronal , Myogenic , and Hepatic Cell Types,
1916 Macromolecular Bioscience. 1800113 (2018) 1–12.
1917 https://doi.org/10.1002/mabi.201800113.

1918 [279] M. Schuster, C. Turecek, B. Kaiser, J. Stampfl, R. Liska, F. Varga, Evaluation of
1919 biocompatible photopolymers I: Photoreactivity and mechanical properties of
1920 reactive diluents, Journal of Macromolecular Science, Part A: Pure and Applied
1921 Chemistry. 44 (2007) 547–557. https://doi.org/10.1080/10601320701235958.

1922 [280] C. Warr, J.C. Valdoz, B.P. Bickham, C.J. Knight, N.A. Franks, N. Chartrand, P.M.
1923 Van Ry, K.A. Christensen, G.P. Nordin, A.D. Cook, Biocompatible PEGDA Resin
1924 for 3D Printing, ACS Applied Bio Materials. 3 (2020) 2239–2244.
1925 https://doi.org/10.1021/acsabm.0c00055.

1926 [281] Y. Zhang, Post-3D printing modification for improved biomedical applications,
1927 International Journal of Bioprinting. 3 (2017).
1928 https://doi.org/10.18063/ijb.2017.02.001.

1929 [282] G. Gonzalez, D. Baruffaldi, C. Martinengo, A. Angelini, A. Chiappone, I. Roppolo,
1930 F.C. Pirri, F. Frascella, Materials Testing for the Development of Biocompatible
1931 Devices through Vat-Polymerization 3D Printing, Nanomaterials. 10 (2020) 1788.
1932 https://doi.org/10.3390/nano10091788.

1933 [283] X. Wang, X. Cai, Q. Guo, T. Zhang, B. Kobe, J. Yang, I3DP, a robust 3D printing
1934 approach enabling genetic post-printing surface modification, Chemical
1935 Communications. 49 (2013) 10064–10066. https://doi.org/10.1039/c3cc45817b.

1936 [284] A. Chiadò, G. Palmara, A. Chiappone, C. Tanzanu, C.F. Pirri, I. Roppolo, F.
1937 Frascella, A modular 3D printed lab-on-a-chip for early cancer detection, Lab on
1938 a Chip. 20 (2020) 665–674. https://doi.org/10.1039/c9lc01108k.

1939 [285] J.A. Calvo-Haro, J. Pascau, J.M. Asencio-Pascual, F. Calvo-Manuel, M.J. Cancho-
1940 Gil, J.F. Del Cañizo López, M. Fanjul-Gómez, R. García-Leal, G. González-
1941 Casaurrán, M. González-Leyte, J.A. León-Luis, L. Mediavilla-Santos, S.
1942 Ochandiano-Caicoya, R. Pérez-Caballero, A. Ribed-Sánchez, J. Río-Gómez, E.
1943 Sánchez-Pérez, J. Serrano-Andreu, M. Tousidonis-Rial, J. Vaquero-Martín, S.
1944 García San José, R. Perez-Mañanes, Point-of-care manufacturing: a single
1945 university hospital's initial experience, 3D Printing in Medicine. 7 (2021) 1–14.
1946 https://doi.org/10.1186/s41205-021-00101-z.

1947 [286] H.N. Chan, M.J.A. Tan, H. Wu, Point-of-care testing: Applications of 3D printing,
1948 Lab on a Chip. 17 (2017) 2713–2739. https://doi.org/10.1039/c7lc00397h.

1949 [287] D. Wang, H.N. Chan, Z. Liu, S. Micheal, L. Li, D.B. Baniani, M.J.A. Tan, L. Huang,
1950 J. Wang, H. Wu, Recent Developments in Microfluidic -Based Point-of-care
1951 Testing (POCT) Diagnoses, 2020. https://doi.org/10.1002/9783527818341.ch8.

1952 [288] C. Tzivelekis, P. Sgardelis, K. Waldron, R. Whalley, D. Huo, K. Dalgarno,
1953 Fabrication routes via projection stereolithography for 3D-printing of
1954 microfluidic geometries for nucleic acid amplification, PLoS ONE. 15 (2020) 1–21.
1955 https://doi.org/10.1371/journal.pone.0240237.

1956 [289] K. Kadimisetty, J. Song, A.M. Doto, Y. Hwang, J. Peng, M.G. Mauk, F.D.
1957 Bushman, R. Gross, J.N. Jarvis, C. Liu, Fully 3D printed integrated reactor array
1958 for point-of-care molecular diagnostics, Biosensors and Bioelectronics. 109 (2018)
1959 156–163. https://doi.org/10.1016/j.bios.2018.03.009.

1960